Acknowledgments

We thank Drs Kenichi Imadome and Shigeyoshi Fujiwara for reagents. We also thank Dr Bill Sugden for critically reading the manuscript. This work was supported by the Japan Health Science Foundation, the Ministry of Health, Labor and Welfare of Japan, and the Ministry of Education, Culture, Sports, Science and Technology of Japan.

Disclosure Statement

The authors have no conflict of interest.

References

1 Thompson MP, Kurzrock R. Epstein–Barr virus and cancer. *Clin Cancer Res* 2004; **10**: 803–21.
2 Rickinson AB, Kieff E. Epstin–Barr virus. In: Knipe DM, Howley PM, eds. *Fields Virology*, 5th edn, vol. 2. Philadelphia: Lippincott Williams & Wilkins, 2007; 2655–700.
3 Klein E, Kis LL, Klein G. Epstein–Barr virus infection in humans: from harmless to life endangering virus-lymphocyte interactions. *Oncogene* 2007; **26**: 1297–305.
4 Snow AL, Martinez OM. Epstein–Barr virus: evasive maneuvers in the development of PTLD. *Am J Transplant* 2007; **7**: 271–7.
5 Besson C, Goubar A, Gabarre J *et al.* Changes in AIDS-related lymphoma since the era of highly active antiretroviral therapy. *Blood* 2001; **98**: 2339–44.
6 Carbone A, Cesarman E, Spina M, Gloghini A, Schulz TF. HIV-associated lymphomas and gamma-herpesviruses. *Blood* 2009; **113**: 1213–24.
7 Kieff E, Rickinson AB. Epstin–Barr virus and its replication. In: Knipe DM, Howley PM, eds. *Fields Virology*, 5th edn, vol. 2. Philadelphia: Lippincott Williams & Wilkins, 2007; 2603–54.
8 Lindner SE, Sugden B. The plasmid replicon of Epstein–Barr virus: mechanistic insights into efficient, licensed, extrachromosomal replication in human cells. *Plasmid* 2007; **58**: 1–12.
9 Wang J, Sugden B. Origins of bidirectional replication of Epstein–Barr virus: models for understanding mammalian origins of DNA synthesis. *J Cell Biochem* 2005; **94**: 247–56.
10 Kirchmaier AL, Sugden B. Plasmid maintenance of derivatives of oriP of Epstein–Barr virus. *J Virol* 1995; **69**: 1280–3.
11 Sugden B, Warren N. Plasmid origin of replication of Epstein–Barr virus, oriP, does not limit replication in cis. *Mol Biol Med* 1988; **5**: 85–94.
12 Leight ER, Sugden B. Establishment of an oriP replicon is dependent upon an infrequent, epigenetic event. *Mol Cell Biol* 2001; **21**: 4149–61.
13 Hurley EA, Thorley-Lawson DA. B cell activation and the establishment of Epstein–Barr virus latency. *J Exp Med* 1988; **168**: 2059–75.
14 Altmann M, Pich D, Ruiss R, Wang J, Sugden B, Hammerschmidt W. Transcriptional activation by EBV nuclear antigen 1 is essential for the expression of EBV's transforming genes. *Proc Natl Acad Sci U S A* 2006; **103**: 14188–93.
15 Kennedy G, Komano J, Sugden B. Epstein–Barr virus provides a survival factor to Burkitt's lymphomas. *Proc Natl Acad Sci U S A* 2003; **100**: 14269–74.
16 Nasimuzzaman M, Kuroda M, Dohno S *et al.* Eradication of Epstein–Barr virus episome and associated inhibition of infected tumor cell growth by adenovirus vector-mediated transduction of dominant-negative EBNA1. *Mol Ther* 2005; **11**: 578–90.
17 Kirchmaier AL, Sugden B. Dominant-negative inhibitors of EBNA-1 of Epstein–Barr virus. *J Virol* 1997; **71**: 1766–75.
18 Komano J, Miyauchi K, Matsuda Z, Yamamoto N. Inhibiting the Arp2/3 complex limits infection of both intracellular mature vaccinia virus and primate lentiviruses. *Mol Biol Cell* 2004; **15**: 5197–207.
19 Aiyar A, Sugden B. Fusions between Epstein–Barr viral nuclear antigen-1 of Epstein–Barr virus and the large T-antigen of simian virus 40 replicate their cognate origins. *J Biol Chem* 1998; **273**: 33073–81.
20 Middleton T, Sugden B. EBNA1 can link the enhancer element to the initiator element of the Epstein–Barr virus plasmid origin of DNA replication. *J Virol* 1992; **66**: 489–95.
21 Urano E, Kariya Y, Futahashi Y *et al.* Identification of the P-TEFb complex-interacting domain of Brd4 as an inhibitor of HIV-1 replication by functional cDNA library screening in MT-4 cells. *FEBS Lett* 2008; **582**: 4053–8.
22 Shimizu S, Urano E, Futahashi Y *et al.* Inhibiting lentiviral replication by HEXIM1, a cellular negative regulator of the CDK9/cyclin T complex. *AIDS* 2007; **21**: 575–82.
23 Kanda T, Yajima M, Ahsan N, Tanaka M, Takada K. Production of high-titer Epstein–Barr virus recombinants derived from Akata cells by using a bacterial artificial chromosome system. *J Virol* 2004; **78**: 7004–15.
24 Mackey D, Sugden B. The linking regions of EBNA1 are essential for its support of replication and transcription. *Mol Cell Biol* 1999; **19**: 3349–59.
25 Howe JG, Shu MD. Epstein–Barr virus small RNA (EBER) genes: unique transcription units that combine RNA polymerase II and III promoter elements. *Cell* 1989; **57**: 825–34.
26 Yajima M, Imadome K, Nakagawa A *et al.* A new humanized mouse model of Epstein–Barr virus infection that reproduces persistent infection, lymphoproliferative disorder, and cell-mediated and humoral immune responses. *J Infect Dis* 2008; **198**: 673–82.

Journal of General Virology (2010), **91**, 42–50 DOI 10.1099/vir.0.013482-0

Quantitative analysis of Epstein–Barr virus (EBV)-related gene expression in patients with chronic active EBV infection

Seiko Iwata,[1] Kaoru Wada,[1] Satomi Tobita,[1] Kensei Gotoh,[2] Yoshinori Ito,[2] Ayako Demachi-Okamura,[3] Norio Shimizu,[4] Yukihiro Nishiyama[1] and Hiroshi Kimura[1]

Correspondence
Hiroshi Kimura
hkimura@med.nagoya-u.ac.jp

[1]Department of Virology, Nagoya University Graduate School of Medicine, Nagoya, Japan

[2]Department of Pediatrics, Nagoya University Graduate School of Medicine, Nagoya, Japan

[3]Division of Immunology, Aichi Cancer Center Research Institute, Nagoya, Japan

[4]Department of Virology, Division of Medical Science, Medical Research Institute, Graduate School of Medicine, Tokyo Medical and Dental University, Tokyo, Japan

Chronic active Epstein–Barr virus (CAEBV) infection is a systemic Epstein–Barr virus (EBV)-positive lymphoproliferative disorder characterized by persistent or recurrent infectious mononucleosis-like symptoms in patients with no known immunodeficiency. The detailed pathogenesis of the disease is unknown and no standard treatment regimen has been developed. EBV gene expression was analysed in peripheral blood samples collected from 24 patients with CAEBV infection. The expression levels of six latent and two lytic EBV genes were quantified by real-time RT-PCR. EBV-encoded small RNA 1 and *Bam*HI-A rightward transcripts were abundantly detected in all patients, and latent membrane protein (LMP) 2 was observed in most patients. EBV nuclear antigen (EBNA) 1 and LMP1 were detected less frequently and were expressed at lower levels. EBNA2 and the two lytic genes were not detected in any of the patients. The pattern of latent gene expression was determined to be latency type II. EBNA1 was detected more frequently and at higher levels in the clinically active patients. Quantifying EBV gene expression is useful in clarifying the pathogenesis of CAEBV infection and may provide information regarding a patient's disease prognosis, as well as possible therapeutic interventions.

Received 22 May 2009
Accepted 25 September 2009

INTRODUCTION

Epstein–Barr virus (EBV) is the causative agent of infectious mononucleosis and is associated with several malignancies, including Burkitt's lymphoma, Hodgkin's lymphoma, nasopharyngeal carcinoma and post-transplant lymphoproliferative disorders (Cohen, 2000; Rickinson & Kieff, 2007; Williams & Crawford, 2006). Chronic active EBV (CAEBV) infection is a systemic EBV-positive lymphoproliferative disorder characterized by persistent or recurrent infectious mononucleosis-like symptoms in patients with no known immunodeficiency (Kimura, 2006; Okano *et al.*, 2005; Straus, 1988; Tosato *et al.*, 1985). The clonal expansion of EBV-infected T cells or natural killer (NK) cells plays a pathogenic role in patients with CAEBV, particularly among those in east Asia or central America (Kanegane *et al.*, 2002; Kimura, 2006; Quintanilla-Martinez *et al.*, 2000). These patients can be classified into two groups based on the predominantly infected cell type, T cells or NK cells (Kimura *et al.*, 2001, 2003). Nonetheless, the detailed pathogenesis of CAEBV remains elusive and no standard treatment regimen has been developed. Recently, haematopoietic stem cell transplantation (HSCT) was introduced as a curative therapy for CAEBV (Fujii *et al.*, 2000; Okamura *et al.*, 2000; Taketani *et al.*, 2002); however, transplant-related complications are common in such patients (Gotoh *et al.*, 2008; Kimura *et al.*, 2001, 2003). Alternatively, the EBV-related antigens expressed by infected cells are possible targets for treatment with EBV-specific cytotoxic T lymphocytes (CTLs) (Heslop *et al.*, 1996; Rooney *et al.*, 1998).

Viral gene expression in EBV-associated diseases is classified into one of three latency patterns (Cohen, 2000; Kieff & Rickinson, 2007). Latency type I, which is found in Burkitt's lymphoma, is characterized by EBV nuclear antigen (EBNA) 1, EBV-encoded small RNAs (EBERs) and *Bam*HI-A rightward transcripts (BARTs) expression (Tao *et al.*, 1998). In latency type II, which is characteristic

A supplementary table of primer sequences is available with the online version of this paper.

of Hodgkin's lymphoma and nasopharyngeal carcinoma, EBNA1, latent membrane protein (LMP) 1, LMP2, EBERs and BARTs are expressed (Brooks *et al.*, 1992; Deacon *et al.*, 1993). In latency type III, which is associated with post-transplant lymphoproliferative disorders, all of the above latent genes (EBNA1, EBNA2, EBNA3A, 3B, 3C, EBNA-LP, LMP1, LMP2, EBERs and BARTs) are expressed (Young *et al.*, 1989).

We recently reported that EBV gene expression could be quantitatively assessed by multiplex real-time RT-PCR (Kubota *et al.*, 2008). This method not only helps quantify EBV gene expression but also can be used to clarify the pathogenesis of EBV-associated diseases and to provide information about their prognosis and possible therapeutic interventions. Thus, in this study, we quantified the expression of six latent (EBNA1, EBNA2, LMP1, LMP2, EBER1 and BARTs) and two lytic [BZLF1 and glycoprotein (gp) 350/220] EBV genes in the peripheral blood of patients with CAEBV.

RESULTS

First, we quantified the expression of several EBV genes in B, T and NK cell lines by real-time RT-PCR (Fig. 1a). In the EBV-positive B cell lines (Raji, LCL-1 and LCL-2), all six latent genes (EBNA1, EBNA2, LMP1, LMP2, EBER1 and BARTs) were detected, and the gene expression pattern was consistent with latency type III. Both lytic genes were detected in LCL-1 and -2 cells. However, none of the target genes was detected in BJAB, an EBV-negative cell line. EBNA1, LMP1, LMP2, EBER1 and BARTs, but not EBNA2, were detected in both the T (SNT-8, -13, -15 and -16) and NK cell lines (SNK-1, -6, -10 and KAI-3). The pattern of expression in the T and NK cell lines was latency type II.

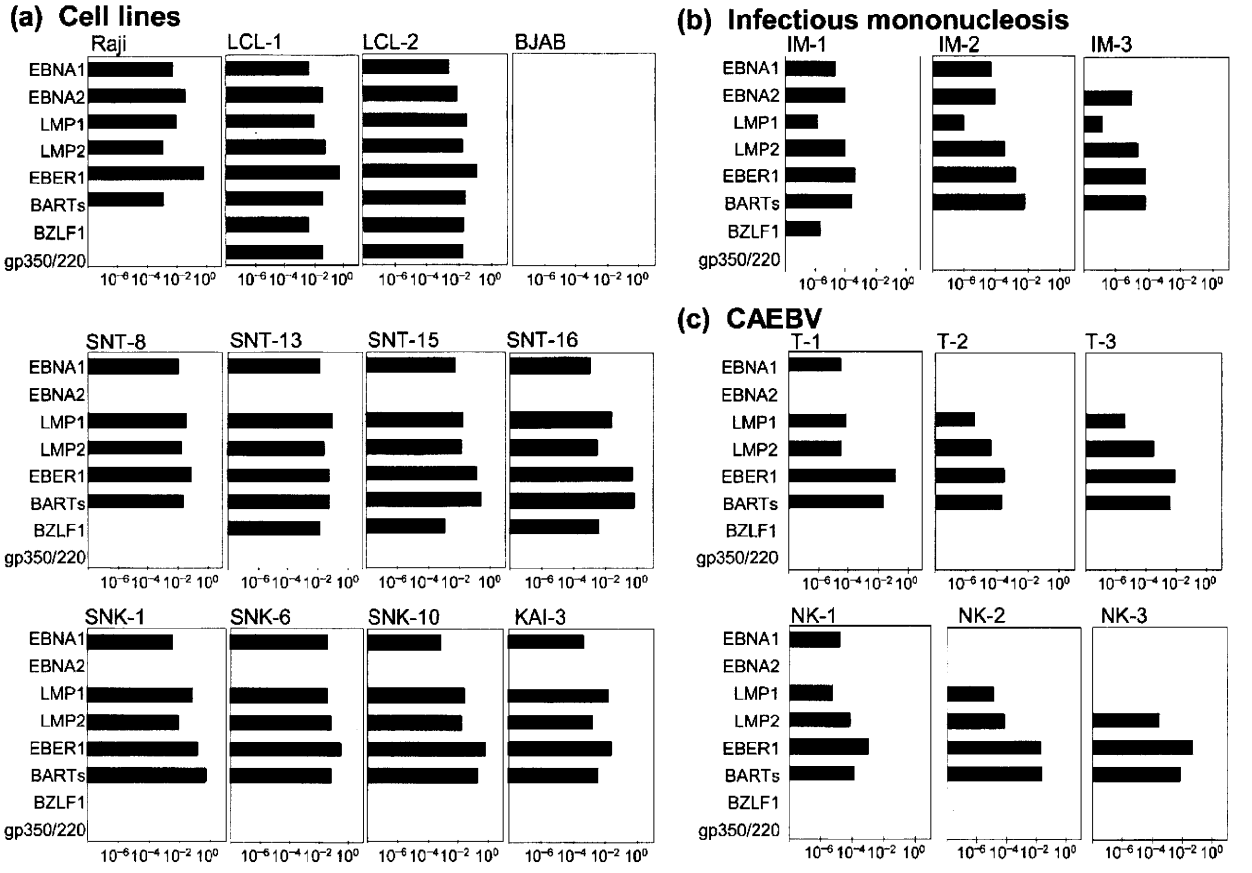

Fig. 1. Analysis of EBV gene expression by real-time RT-PCR. β2-Microglobin (β2 m) was used as an endogenous control and reference gene for relative quantification and was assigned an arbitrary value of 1 (10^0). (a) The quantity of each EBV gene in B, T and NK cells. Raji, LCL-1 and LCL-2 are EBV-positive B cell lines. BJAB is an EBV-negative B cell line. SNT-8, -13, -15 and -16 are EBV-positive T cell lines. SNK-1, -6, -10 and KAI-3 are EBV-positive NK cell lines. (b) Quantitative expression of the EBV genes in patients with infectious mononucleosis. (c) Representative results showing the relative expression of EBV genes in patients with a CAEBV infection. T-1, -2 and -3 are T-cell-type cases (patients 6, 9 and 11 in Table 1), while NK-1, -2 and -3 are NK-cell-type cases (patients 14, 15 and 19 in Table 1).

BZLF1 was detected in three of four T-cell lines, while gp350/220 was not detected in any of the cell lines, indicating an abortive lytic cycle. These results are consistent with those from previous reports (Leenman *et al.*, 2004; Tao *et al.*, 1998; Tsuge *et al.*, 1999; Zhang *et al.*, 2003), indicating the reliability of our system. We evaluated the sensitivity for each latent EBV gene using a cell mixture containing 1×10^6 EBV-negative BJAB cells and 10-fold serial dilutions of LCL-1 with latency III. The detection limits for EBNA1, EBNA2, LMP1, LMP2, EBER1 and BARTs were 0.1, 0.1, 0.01, 0.01, 0.001 and 0.01 % of LCL-1 cells, respectively. To evaluate the sensitivity for lytic genes, cell mixtures containing BJAB and Akata cells with a lytic infection, induced by human immunoglobulin G, were used. The detection limits for BZLF1 and gp350/220 were 0.1 % of Akata cells.

Next, we analysed blood from three patients with acute-phase infectious mononucleosis (Fig. 1b). EBNA2, LMP1, LMP2, EBER1 and BARTs were detected in the PBMCs of the patients, whereas EBNA1 was detected in two patients. The gene expression pattern in each case was latency type III. BZLF1 was detected in one patient, whereas gp350/220 was not detected in any patient. Furthermore, we analysed the PBMCs of 23 healthy carriers. Four healthy carriers were positive for EBV DNA. Real-time RT-PCR detected EBER1 and BARTs in the PBMCs of one carrier, while EBER1 alone was detected in a single additional carrier.

We next quantified the expression level of each gene in 24 patients with CAEBV. PBMCs collected at the time of diagnosis or referral were used in the analysis. The expression profiles of each patient are shown in Table 1, while the positive rates for each EBV gene are summarized in Table 2. EBER1 and BARTs were detected in each patient, while LMP2 was detected in most patients. EBNA1 and LMP1 were detected less frequently compared with EBER1 and BARTs ($P<0.0001$ and $P=0.004$, respectively). EBNA2 and the lytic genes BZLF1 and gp350/220 were undetected in all of the patients. Representative

Table 1. Characteristics and EBV gene expression profiles of 24 patients with chronic active EBV infection

ND, Not done. EBNA2, BZLF1 and gp350/220 were not expressed in any samples. EBER1 and BARTs were expressed in all samples.

Patient	Age (years)	Gender	Cell type infected	Viral load*				Disease type†	HSCT	Outcome	Viral load‡	EBV gene expression		
				PBMC	$CD3^+$	$CD19^+$	$CD56^+$					EBNA1	LMP1	LMP2
1	6	M	T	85925	**157196**	32828	62047	I	−	Alive	241000	−	+	+
2	5	M	T	74915	**119024**	12292	**77651**	I	−	Alive	392203	+	−	+
3	25	M	T	10749	**12106**	2742	5739	I	−	Alive	297	−	−	−
4	10	M	T	18308	**23422**	12665	**27106**	I	−	Alive	19363	−	+	+
5	6	M	T	14162	**22559**	1583	1073	A	+	Alive	14162	−	−	+
6	4	F	T	15776	**17312**	5243	4321	A	+	Alive	15776	+	+	+
7	11	M	T	60097	**143852**	23212	6352	A	+	Alive	60097	−	−	+
8	18	F	T/B	93458	**118026**	**174042**	**267078**	A	+	Alive	392734	+	+	+
9	14	F	T	30633	**32730**	8345	4760	I	+	Alive	30633	−	+	+
10	24	F	T	8589	**43469**	2388	**12555**	A	−	Dead	37148	+	−	+
11	23	F	T	5684	**7990**	4200	250	I	+	Dead	2764	−	+	+
12	13	M	T	3176	**3579**	948	839	I	+	Dead	10681	+	+	+
13	16	F	T	52978	**55431**	37536	**84110**	I	+	Dead	52978	−	+	+
14	11	M	NK	370000	31600	100000	**1800000**	I	−	Alive	339589	+	+	+
15	9	M	NK	77884	7428	17083	**89352**	I	−	Alive	89930	−	+	+
16	4	M	NK	74550	11288	18423	**86361**	A	+	Alive	74550	+	+	+
17	5	F	NK	11200	330	3300	**23400**	A	+	Alive	1108	+	+	+
18	3	M	NK	131957	1591	16450	**917500**	I	+	Alive	131957	−	+	+
19	9	M	NK	263429	92057	206565	**425956**	I	+	Alive	263429	−	−	+
20§	26	F	NK	18889	ND	ND	ND	I	+	Alive	18889	−	+	−
21	14	F	NK	1559	53	105	**4302**	A	−	Dead	1051	−	−	−
22	14	F	NK	20126	3288	1866	**35252**	I	+	Dead	44750	+	+	+
23§	16	M	NK	69121	ND	ND	ND	I	+	Dead	69121	+	+	+
24§	14	F	NK	1041	ND	ND	ND	I	+	Dead	1041	−	−	−

*Bold type indicates that EBV DNA was concentrated by fractionation; copies $(\mu g\ DNA)^{-1}$.

†Patients with severe symptoms were defined as having a clinically active disease (A); patients with no symptoms or with only skin symptoms were defined as having an inactive disease (I).

‡Indicates the EBV DNA in the PBMCs used for real-time RT-PCR analysis; copies $(\mu g\ DNA)^{-1}$.

§Infection was confirmed by *in situ* hybridization with EBER using fractionated cells.

Table 2. Detection of eight EBV-related genes in 24 patients with a CAEBV infection

Gene	No. positive patients (%)	*P*-value*
EBNA1	10 (42)	<0.001
EBNA2	0 (0)	<0.001
LMP1	16 (67)	0.004
LMP2	20 (83)	0.11
EBER1	24 (100)	–
BARTs	24 (100)	–
BZLF1	0 (0)	<0.001
gp350/220	0 (0)	<0.001

*Comparison with EBER1 and BARTs. All *P*-values were obtained using Fisher's exact test.

quantitative results for each EBV gene are shown in Fig. 1(c).

The negative results obtained for EBNA1 and LMP1 raise the possibility that the test was not sensitive enough to detect low levels of expression. Therefore, we examined the correlation between the relative expression level for each gene and the EBV DNA load in the PBMCs (Fig. 2). For all of the EBV genes examined, the expression level correlated with the EBV DNA load. However, the samples with a low EBV DNA load were not always negative for EBNA1; similar findings were seen for LMP1.

To confirm the EBV gene expression profiles in various cell populations, we separated $CD3^+$, $CD19^+$ and $CD56^+$ cells from the PBMCs by immunomagnetic sorting and quantified the gene expression in each population by real-time RT-PCR using selected patients and healthy carriers. In one patient with T-cell-type CAEBV (patient 2 in Table 1; $CD3^+$ $CD56^+$ T cells harboured EBV), type II latent genes, such as EBNA1, LMP2, EBER1 and BARTs, were detected in both the $CD3^+$ and $CD56^+$ cell populations (Fig. 3a). In a patient with NK-cell-type CAEBV (patient 14 in Table 1), type II latent genes were detected primarily in the $CD56^+$ population (Fig. 3b). On the other hand, in a healthy carrier, EBER1 and BARTs were detected in the $CD19^+$ population (presumed to be the B-cell fraction; Fig. 3c). Importantly, the gene expression profiles in the mainly infected cells largely corresponded to those in the unsorted PBMCs in all three cases, suggesting that our PBMC data could be applied to the cells in the mainly infected population.

We next estimated the mean expression level for each EBV gene in 24 patients with CAEBV (Fig. 4a). EBER1 had the highest relative expression level, followed by BARTs, LMP2 and EBNA1, whereas LMP1 had the lowest. Next, we compared the expression level for each EBV gene between the T- and NK-cell types of CAEBV (Fig. 4b). No significant difference was found, although LMP2 expression tended to be higher in the T-cell type ($P=0.09$). We also compared the expression levels between the clinically active patients, who presented with severe symptoms at the time of sample collection, and clinically inactive patients (Fig. 4c). EBNA1 expression was 8.3 times higher in the active patients than in the inactive patients ($P=0.02$). Additionally, the rate of EBNA1-positive patients in the active group was significantly higher (75 versus 25%; $P=0.03$). On the other hand, there was no difference in EBV DNA load in the peripheral blood between the active and inactive groups [$10^{4.4}$ versus $10^{4.5}$ copies $(\mu g\ DNA)^{-1}$; $P=0.85$]. We also investigated whether EBV gene expression at the time of diagnosis or referral to our hospital was associated with the subsequent disease outcome. We divided the patients into three groups: survivors without HSCT, survivors with HSCT and non-survivors. No significant difference was observed in the gene expression profiles of the three groups (Fig. 4d).

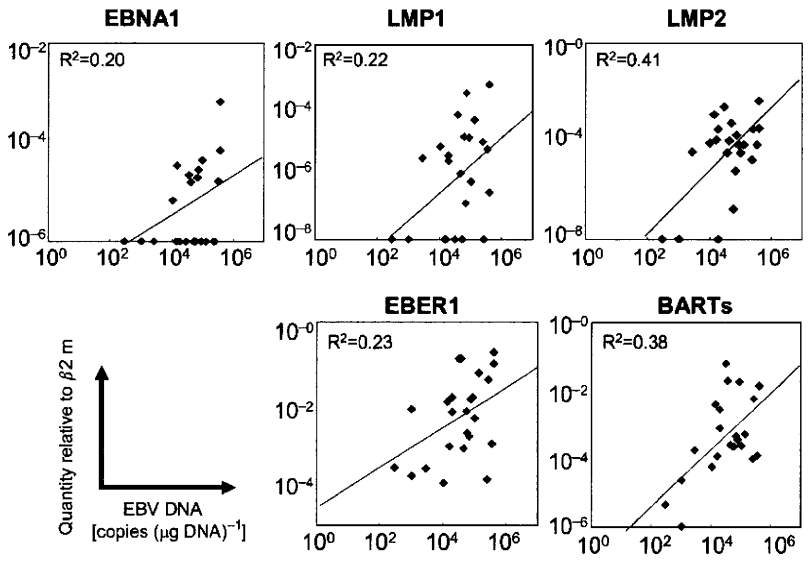

Fig. 2. Relationship between the quantity of each EBV gene and the EBV DNA load in PBMCs from patients with CAEBV. The correlation in all of these was statistically significant.

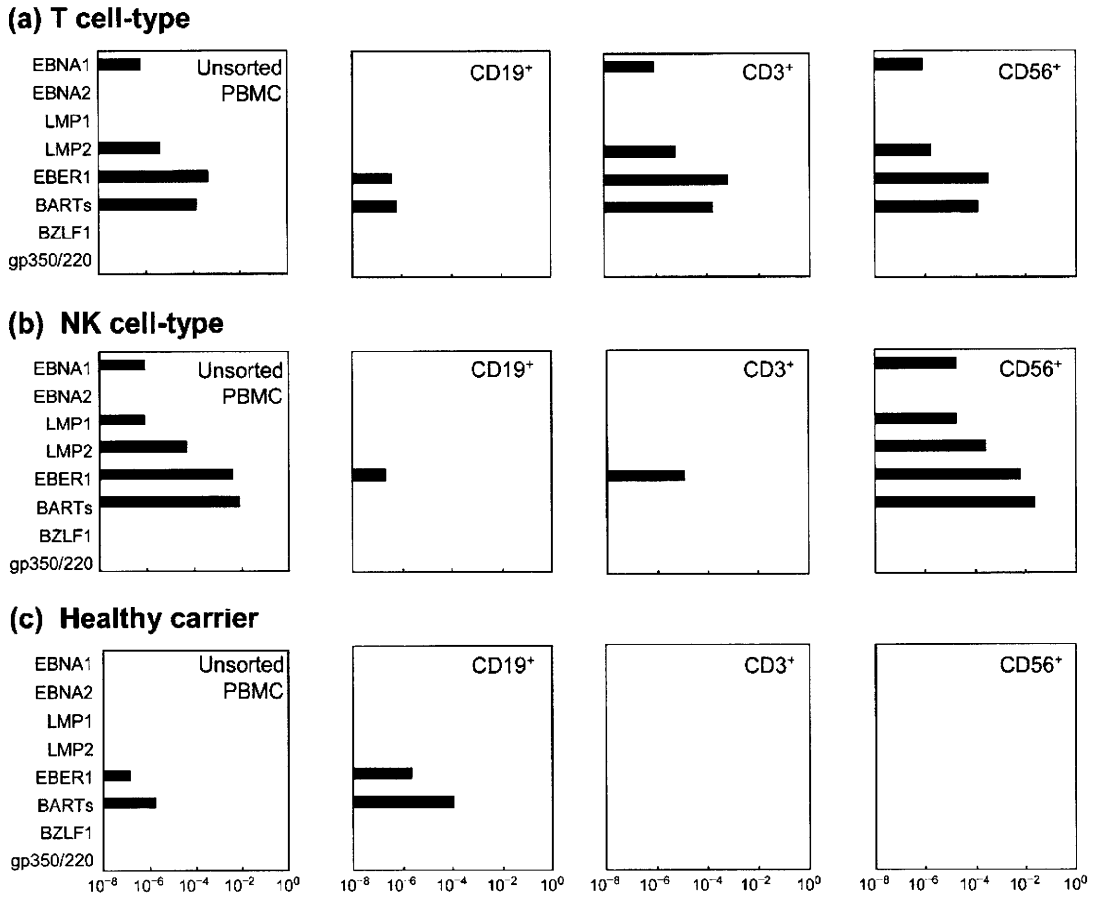

Fig. 3. EBV gene expression in sorted cell populations. $CD19^+$, $CD3^+$ and $CD56^+$ cells were separated by immunomagnetic sorting and analysed by real-time RT-PCR; unsorted PBMCs were analysed. (a) A T-cell-type CAEBV patient (patient 2 in Table 1; $CD3^+$ $CD56^+$ T cells were the main type of infected cells). (b) An NK-cell-type CAEBV patient (patient 14 in Table 1). (c) A healthy carrier whose PBMCs were positive for EBV DNA.

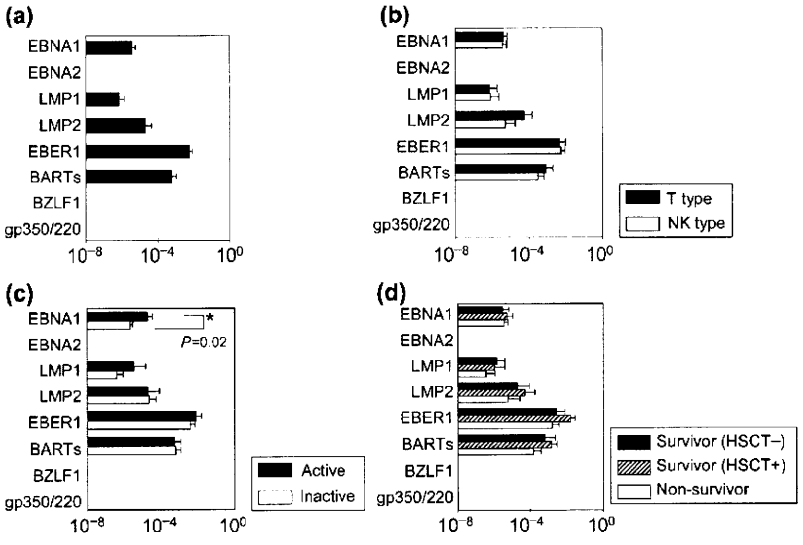

Fig. 4. EBV gene expression profile for patients with CAEBV. The quantity of each EBV gene was analysed by real-time RT-PCR and compared with the $\beta 2$ m level; the mean ± SE (boxes and bars) was calculated for each gene. (a) Average expression of EBV genes in 24 patients with CAEBV. (b) Comparison between T- (13 cases) and NK- (11 cases) cell-types. (c) Comparison between clinically active (8 cases) and inactive (16 cases) patients. (d) Comparisons of surviving patients without HSCT (6 cases), surviving patients with HSCT (10 cases) and non-surviving patients (8 cases). The Mann–Whitney *U*-test was used to compare the expression values between the groups, while the analysis of variance was used to compare the groups of three.

Finally, to eliminate any potential influence of therapeutic interventions, we excluded six patients who had received therapy before entering our hospital and re-evaluated the expression of each gene in the remaining 18 patients. The level of EBNA1 expression in the active patients was 8.2 times higher than that in the inactive patients (P=0.03) and the rate of EBNA1-positive patients was significantly higher in the active group (83 versus 25 %; P=0.04). We also re-evaluated the disease outcome in these 18 patients. No significant difference was observed in the gene expression profiles between the three groups according to outcome (data not shown).

DISCUSSION

Analysing the expression profile of EBV-related genes is essential to clarify the pathogenesis of EBV-associated diseases and to uncover information regarding the prognosis of individual patients and potential therapeutic interventions. In recent years, a quantitative method for the analysis of EBV gene expression has been applied to infectious mononucleosis (Weinberger *et al.*, 2004), Burkitt's lymphoma and nasopharyngeal carcinoma (Bell *et al.*, 2006). In the present study, we quantified the expression of six latent genes and two lytic genes in 24 patients with CAEBV using one-step multiplex real-time RT-PCR. To our knowledge, this is the first study to quantify EBV gene expression in CAEBV patients. EBNA1, LMP1, LMP2, EBER1 and BARTs were detected in the patient samples, whereas EBNA2 and the two lytic genes were not detected. The gene expression pattern was latency type II, consistent with previous qualitative RT-PCR results (Kimura *et al.*, 2005). Because the lytic genes BZLF1 and gp350/220 were undetected, a lytic infection is unlikely in the peripheral blood of the CAEBV patients. EBER1 and BARTs were detected in abundance in all patients, while LMP2 was found in most patients. EBNA1 and LMP1 were less frequently detected and had lower expression levels than EBER1 and BARTs. These results are in contrast with similar analyses using T or NK cell lines, in which EBNA1, LMP1, LMP2, EBER1 and BARTs were abundantly and comparably expressed. EBNA1, EBNA2 and EBNA3C are the dominant targets of $CD4^+$ T-cell responses, while EBNA3A, EBNA3B and EBNA3C are the dominant targets of $CD8^+$ T-cell responses (Hislop *et al.*, 2007). In those patients with CAEBV, most or all of these antigens were not expressed, contributing to the evasion of cellular immunity. The decreased frequency and low expression level of EBNA1 may also contribute to the immunological escape mechanism of CAEBV.

The expression profile identified in this study may be useful for obtaining information regarding potential immunotherapies. The EBV-related antigens expressed by infected cells are possible targets for treatment with EBV-specific CTLs. Several studies have reported the use of such therapies for CAEBV, but most have shown only limited effectiveness (Hagihara *et al.*, 2003; Kuzushima *et al.*, 1996; Savoldo *et al.*, 2002). These studies used EBV-specific CTLs that were generated from LCL and targeted latency type III antigens. Our results indicate that EBER1 and BARTs were the most frequently and abundantly expressed EBV genes, followed by LMP2. Because very little EBER1 and BARTs mRNA is translated into protein (Arrand & Rymo, 1982; Kieff & Rickinson, 2007), LMP2 would be the most favourable target for CTL therapy against CAEBV. Recently, EBV-specific CTLs targeted against LMP2 were used to treat Hodgkin's lymphoma and nasopharyngeal carcinoma, both of which are latency type II infections (Bollard *et al.*, 2004, 2007; Straathof *et al.*, 2005). Furthermore, patients with CAEBV generally lack LMP2-specific CTLs (Sugaya *et al.*, 2004). However, to develop effective and useful forms of immunotherapy, additional studies focusing on the nature of the infected cells and the underlying pathology of CAEBV are necessary.

In this study, we quantified the relative expression of EBV latent and lytic genes by real-time RT-PCR. There are a few drawbacks to our system. Firstly, we used β2-microglobulin (β2 m) as a reference for relative quantification; however, comparisons of the levels of expression between different genes may be compromised by variations in the efficiency of the primers used. Another option for such quantification is preparing a standard curve for each cDNA by diluting the plasmid and estimating the number of RNA copies to quantify the expression of each gene more accurately. Secondly, we determined the type of latency based on the patterns of viral gene expression. Promoter usage for EBNA1 is different between latency types I/II and III (Qp versus Cp) (Kieff & Rickinson, 2007). Primers capable of distinguishing between the two EBNA1 promoters would enable us to confirm the type of latency more accurately. Bell *et al.* (2006) used such a system to distinguish latency types and quantify gene expression using different EBNA1 primers.

There are several possible reasons why EBNA1 and LMP1 were detected less frequently in our analysis. First, EBV-infected T or NK cells in some patients with CAEBV may indeed express very little LMP1 or EBNA1. A previous experiment performed using nested RT-PCR, which is sensitive but not quantitative, showed that these genes were expressed in less than half of CAEBV patients (Kimura *et al.*, 2005). Second, the sensitivity of the test may be too low to detect these genes. However, those samples with a low EBV DNA load in this study were not always negative for EBNA1 or LMP1, indicating that low sensitivity was not the only reason that the expression of these genes was not detected. Moreover, EBV polymorphisms may have affected our results. Indeed, the primers used for LMP1 are specific for polymorphic regions (Kubota *et al.*, 2008). However, we used mixed primers for LMP1 to account for sequence variations, and the EBNA1 primers were designed to recognize fairly conserved regions. Furthermore, we also examined EBNA1- or LMP1-negative samples by nested RT-PCR using alternate primer sets (Kimura *et al.*, 2005).

Neither EBNA1 nor LMP1 was detected in any of the samples by nested PCR (data not shown).

EBNA1 was detected more frequently and abundantly in the clinically active patients. EBNA1 is the only EBV protein consistently expressed in all proliferating cells, and it plays central roles in the maintenance and replication of the episomal EBV genome. EBNA1 also has a role in cell growth and survival (Kieff & Rickinson, 2007; Thorley-Lawson & Gross, 2004). Recently, Saridakis *et al.* (2005) demonstrated that EBNA1 inhibits apoptosis by binding to USP7, which destabilizes p53. Together with our results, these findings suggest that EBNA1 plays an important part in the pathogenesis and symptoms of CAEBV.

EBV gene expression has been shown to be related to the prognosis of EBV-associated diseases. Kwon *et al.* (2006) evaluated EBER and LMP1 expression in patients with Hodgkin's lymphoma, while Tsang *et al.* (2003) reported a relationship between the recurrence and detection of LMP1 in patients with nasopharyngeal carcinoma. Similarly, we evaluated the relationship between EBV gene expression and the prognosis of CAEBV, but were unable to identify a significant link. Other factors that may have influenced the results of this study include the small sample size, short observation period and therapeutic interventions such as HSCT. Additional studies with a greater number of cases and a longer observation period are necessary to reach conclusions about the prognostic value of EBV gene quantification for CAEBV. In conclusion, we applied a real-time RT-PCR system to PBMCs from patients with CAEBV and identified the expression profiles of several EBV genes. Quantifying EBV gene expression may be useful in clarifying CAEBV pathogenesis and provide further information about therapeutic interventions, such as CTL therapy.

METHODS

Cell lines. The EBV-positive B cell lines used in this study were Raji, Akata, lymphoblastoid cell line (LCL)-1 and LCL-2. BJAB, an EBV-negative B cell line, was used as a negative control. The EBV-positive T cell lines used were SNT-8, -13, -15 and -16 (Zhang *et al.*, 2003). The EBV-positive NK cell lines used were SNK-1, -6 and -10 (Zhang *et al.*, 2003) and KAI-3 (Tsuge *et al.*, 1999). The T/NK cell lines were derived from patients with CAEBV or nasal NK-/T-cell lymphomas.

Patients. Twenty-four patients (13 males and 11 females) with CAEBV, ranging in age from 3 to 26 years (median age 13 years), were enrolled in this study (Table 1). Each patient met the following diagnostic criteria: EBV-related symptoms for at least 6 months (e.g. fever, persistent hepatitis, extensive lymphadenopathy, hepatosplenomegaly, pancytopenia, uveitis, interstitial pneumonia, hydroa vacciniforme or hypersensitivity to mosquito bites), an increased EBV load in either the affected tissue or peripheral blood, and no evidence of previous immunological abnormalities or other recent infections that could explain the condition (Kimura, 2006; Kimura *et al.*, 2001). Based on the infected cell type, 13 patients were identified as having T-cell-type CAEBV, while 11 were identified as having NK-cell-type CAEBV. To determine which cells harboured the most EBV, peripheral blood mononuclear cells (PBMCs) were fractionated into $CD3^+$, $CD19^+$ and $CD56^+$ cells and analysed by either quantitative PCR or *in situ* hybridization, using EBER1 as a probe, as described previously (Kimura *et al.*, 2001, 2005). The patients were defined as having a T-cell-type infection if their $CD3^+$ cells contained larger amounts of EBV DNA than their PBMCs, or if their $CD3^+$ cells gave a positive hybridization signal with EBER1. The patients were defined as having an NK-cell-type infection if their $CD56^+$ cells, rather than their $CD3^+$ cells, were the major cells harbouring EBV. The EBV DNA copy numbers in each cell population are shown in Table 1.

Peripheral blood was collected at the time of diagnosis or referral to our hospital. Six of 24 patients had already received steroid therapy or chemotherapy. PBMCs were isolated using Ficoll–Paque density gradients (Pharmacia Biotech) and stored at −80 °C until further use. Eight patients with severe symptoms such as high fever, distinct hepatosplenomegaly, and/or elevated hepatic transaminase levels at the time of sample collection were defined as having clinically active disease, while 16 patients with no symptoms or with only skin symptoms, including hydroa vacciniforme, were defined as having inactive disease. Eight of the patients died after 1–49 months of observation (median 14 months). Sixteen of the patients, 10 of whom received HSCT, were alive after 9–115 months of observation (median 28 months). Twenty-three healthy carrier volunteers who were seropositive for EBV and three patients with infectious mononucleosis (aged 5, 11 and 29 years) were enrolled as controls.

Informed consent was obtained from all patients or their guardians. The institutional review board of Nagoya University Hospital approved the use of the specimens that were examined in this study.

Real-time PCR assay. DNA was extracted from 1×10^6 PBMCs using a QIAmp blood mini kit (Qiagen). EBV DNA was quantified by real-time PCR as described previously. The viral load is expressed as the number of copies $(\mu g\ DNA)^{-1}$ (Kimura *et al.*, 1999).

RNA was extracted from 1×10^6 cells using a QIAmp RNeasy mini kit (Qiagen). Contaminating DNA was removed by on-column DNase digestion using the RNase-free DNase set (Qiagen) (Kubota *et al.*, 2008). Viral mRNA expression was quantified by one-step multiplex real-time RT-PCR using an Mx3000P real-time PCR system (Stratagene) as described previously (Kubota *et al.*, 2008). All of the primer/probe combinations, except those for EBER1 lacking an intron, were designed to span introns to avoid amplifying residual genomic DNA. The primer and probe sequences are listed in Supplementary Table S1 (available in JGV Online). The primers used for EBNA1, EBNA2, LMP1 and BZLF1, which were described previously (Kubota *et al.*, 2008), were modified according to sequence variations amongst the strains. The stably expressed housekeeping gene $\beta 2$ m was used as an endogenous control and reference gene for relative quantification (Patel *et al.*, 2004).

Cell sorting and gene expression analysis. $CD3^+$, $CD19^+$ and $CD56^+$ cells were separated from 1×10^7 PBMCs by immunomagnetic sorting using anti-CD3, -CD19 and -CD56 MACS Microbeads, respectively (Miltenyi Biotec). After two rounds of sorting, the purity of the populations exceeded 95 %. RNA was extracted from each cell population for real-time RT-PCR analysis. For comparison, RNA was also extracted from unsorted PBMCs.

Statistical analyses. All statistical analyses were performed using StatView (version 5.0; SAS Institute). Geometric (logarithmic) means were calculated for the expression of each EBV gene. For the negative samples, the default value, which was defined as the lowest level of expression for a particular gene, was used for the calculation. The default values for the undetected genes EBNA1, LMP1 and LMP2 were 10^{-6}, 10^{-8} and 10^{-8}, respectively. The Mann–Whitney *U*-test was used to compare the expression levels between groups, while analysis of variance was used to compare three groups. Fisher's exact

test was used to compare positive rates of gene expression. A regression analysis was used to compare the expression of each gene and the EBV DNA load. *P*-values <0.05 were deemed to be statistically significant.

ACKNOWLEDGEMENTS

We thank the following people for their contributions to this study: Kayoko Matsunaga (Fujita Health University); Masaki Ito, Atsushi Kikuta, and Mitsuaki Hosoya (Fukushima Medical University); Tomohiro Kinoshita (Nagoya University); Kazuhiko Shirota (National Hospital Organization Shizuoka Medical Center); Mariko Seishima (Ogaki Municipal Hispital); Masashi Shiomi (Osaka City General Hospital); Hajime Katsumata and Yasuo Horikoshi (Shizuoka Children's Hospital); Tsuyoshi Ito (Toyohashi City Hospital); and Sachiyo Kamimura (University of Miyazaki). This study was supported in part by a grant from the Ministry of Education, Culture, Sports, Science and Technology, Japan (19591247).

REFERENCES

Arrand, J. R. & Rymo, L. (1982). Characterization of the major Epstein–Barr virus-specific RNA in Burkitt lymphoma-derived cells. *J Virol* **41**, 376–389.

Bell, A. I., Groves, K., Kelly, G. L., Croom-Carter, D., Hui, E., Chan, A. T. & Rickinson, A. B. (2006). Analysis of Epstein–Barr virus latent gene expression in endemic Burkitt's lymphoma and nasopharyngeal carcinoma tumour cells by using quantitative real-time PCR assays. *J Gen Virol* **87**, 2885–2890.

Bollard, C. M., Aguilar, L., Straathof, K. C., Gahn, B., Huls, M. H., Rousseau, A., Sixbey, J., Gresik, M. V., Carrum, G. & other authors (2004). Cytotoxic T lymphocyte therapy for Epstein–Barr virus$^+$ Hodgkin's disease. *J Exp Med* **200**, 1623–1633.

Bollard, C. M., Gottschalk, S., Leen, A. M., Weiss, H., Straathof, K. C., Carrum, G., Khalil, M., Wu, M. F., Huls, M. H. & other authors (2007). Complete responses of relapsed lymphoma following genetic modification of tumor-antigen presenting cells and T-lymphocyte transfer. *Blood* **110**, 2838–2845.

Brooks, L., Yao, Q. Y., Rickinson, A. B. & Young, L. S. (1992). Epstein–Barr virus latent gene transcription in nasopharyngeal carcinoma cells: coexpression of EBNA1, LMP1, and LMP2 transcripts. *J Virol* **66**, 2689–2697.

Cohen, J. I. (2000). Epstein–Barr virus infection. *N Engl J Med* **343**, 481–492.

Deacon, E. M., Pallesen, G., Niedobitek, G., Crocker, J., Brooks, L., Rickinson, A. B. & Young, L. S. (1993). Epstein–Barr virus and Hodgkin's disease: transcriptional analysis of virus latency in the malignant cells. *J Exp Med* **177**, 339–349.

Fujii, N., Takenaka, K., Hiraki, A., Maeda, Y., Ikeda, K., Shinagawa, K., Ashiba, A., Munemasa, M., Sunami, K. & other authors (2000). Allogeneic peripheral blood stem cell transplantation for the treatment of chronic active Epstein-Barr virus infection. *Bone Marrow Transplant* **26**, 805–808.

Gotoh, K., Ito, Y., Shibata-Watanabe, Y., Kawada, J., Takahashi, Y., Yagasaki, H., Kojima, S., Nishiyama, Y. & Kimura, H. (2008). Clinical and virological characteristics of 15 patients with chronic active Epstein–Barr virus infection treated with hematopoietic stem cell transplantation. *Clin Infect Dis* **46**, 1525–1534.

Hagihara, M., Tsuchiya, T., Hyodo, O., Ueda, Y., Tazume, K., Masui, A., Kanemura, A., Yoshiba, F., Takashimizu, S. & other authors (2003). Clinical effects of infusing anti-Epstein–Barr virus (EBV)-specific cytotoxic T-lymphocytes into patients with severe chronic active EBV infection. *Int J Hematol* **78**, 62–68.

Heslop, H. E., Ng, C. Y., Li, C., Smith, C. A., Loftin, S. K., Krance, R. A., Brenner, M. K. & Rooney, C. M. (1996). Long-term restoration of immunity against Epstein–Barr virus infection by adoptive transfer of gene-modified virus-specific T lymphocytes. *Nat Med* **2**, 551–555.

Hislop, A. D., Taylor, G. S., Sauce, D. & Rickinson, A. B. (2007). Cellular responses to viral infection in humans: lessons from Epstein–Barr virus. *Annu Rev Immunol* **25**, 587–617.

Kanegane, H., Nomura, K., Miyawaki, T. & Tosato, G. (2002). Biological aspects of Epstein–Barr virus (EBV)-infected lymphocytes in chronic active EBV infection and associated malignancies. *Crit Rev Oncol Hematol* **44**, 239–249.

Kieff, E. D. & Rickinson, A. V. (2007). Epstein–Barr virus and its replication. In *Fields Virology*, pp. 2603–2654. Edited by D. M. Knipe & P. M. Howley. Philadelphia: Lippincott Williams & Wilkins.

Kimura, H. (2006). Pathogenesis of chronic active Epstein–Barr virus infection: is this an infectious disease, lymphoproliferative disorder, or immunodeficiency? *Rev Med Virol* **16**, 251–261.

Kimura, H., Morita, M., Yabuta, Y., Kuzushima, K., Kato, K., Kojima, S., Matsuyama, T. & Morishima, T. (1999). Quantitative analysis of Epstein–Barr virus load by using a real-time PCR assay. *J Clin Microbiol* **37**, 132–136.

Kimura, H., Hoshino, Y., Kanegane, H., Tsuge, I., Okamura, T., Kawa, K. & Morishima, T. (2001). Clinical and virologic characteristics of chronic active Epstein-Barr virus infection. *Blood* **98**, 280–286.

Kimura, H., Morishima, T., Kanegane, H., Ohga, S., Hoshino, Y., Maeda, A., Imai, S., Okano, M., Morio, T. & other authors (2003). Prognostic factors for chronic active Epstein–Barr virus infection. *J Infect Dis* **187**, 527–533.

Kimura, H., Hoshino, Y., Hara, S., Sugaya, N., Kawada, J., Shibata, Y., Kojima, S., Nagasaka, T., Kuzushima, K. & Morishima, T. (2005). Differences between T cell-type and natural killer cell-type chronic active Epstein–Barr virus infection. *J Infect Dis* **191**, 531–539.

Kubota, N., Wada, K., Ito, Y., Shimoyama, Y., Nakamura, S., Nishiyama, Y. & Kimura, H. (2008). One-step multiplex real-time PCR assay to analyse the latency patterns of Epstein–Barr virus infection. *J Virol Methods* **147**, 26–36.

Kuzushima, K., Yamamoto, M., Kimura, H., Ando, Y., Kudo, T., Tsuge, I. & Morishima, T. (1996). Establishment of anti-Epstein–Barr virus (EBV) cellular immunity by adoptive transfer of virus-specific cytotoxic T lymphocytes from an HLA-matched sibling to a patient with severe chronic active EBV infection. *Clin Exp Immunol* **103**, 192–198.

Kwon, J. M., Park, Y. H., Kang, J. H., Kim, K., Ko, Y. H., Ryoo, B. Y., Lee, S. S., Lee, S. I., Koo, H. H. & Kim, W. S. (2006). The effect of Epstein–Barr virus status on clinical outcome in Hodgkin's lymphoma. *Ann Hematol* **85**, 463–468.

Leenman, E. E., Panzer-Grumayer, R. E., Fischer, S., Leitch, H. A., Horsman, D. E., Lion, T., Gadner, H., Ambros, P. F. & Lestou, V. S. (2004). Rapid determination of Epstein–Barr virus latent or lytic infection in single human cells using *in situ* hybridization. *Mod Pathol* **17**, 1564–1572.

Okamura, T., Hatsukawa, Y., Arai, H., Inoue, M. & Kawa, K. (2000). Blood stem-cell transplantation for chronic active Epstein–Barr virus with lymphoproliferation. *Lancet* **356**, 223–224.

Okano, M., Kawa, K., Kimura, H., Yachie, A., Wakiguchi, H., Maeda, A., Imai, S., Ohga, S., Kanegane, H. & other authors (2005). Proposed guidelines for diagnosing chronic active Epstein–Barr virus infection. *Am J Hematol* **80**, 64–69.

Patel, K., Whelan, P. J., Prescott, S., Brownhill, S. C., Johnston, C. F., Selby, P. J. & Burchill, S. A. (2004). The use of real-time reverse

transcription-PCR for prostate-specific antigen mRNA to discriminate between blood samples from healthy volunteers and from patients with metastatic prostate cancer. *Clin Cancer Res* **10**, 7511–7519.

Quintanilla-Martinez, L., Kumar, S., Fend, F., Reyes, E., Teruya-Feldstein, J., Kingma, D. W., Sorbara, L., Raffeld, M., Straus, S. E. & Jaffe, E. S. (2000). Fulminant EBV(+) T-cell lymphoproliferative disorder following acute/chronic EBV infection: a distinct clinicopathologic syndrome. *Blood* **96**, 443–451.

Rickinson, A. B. & Kieff, E. (2007). Epstein–Barr virus. In *Fields Virology*, pp. 2655–2700. Edited by D. M. Knipe & P. M. Howley. Philadelphia: Lippincott Williams & Wilkins.

Rooney, C. M., Smith, C. A., Ng, C. Y., Loftin, S. K., Sixbey, J. W., Gan, Y., Srivastava, D. K., Bowman, L. C., Krance, R. A. & other authors (1998). Infusion of cytotoxic T cells for the prevention and treatment of Epstein–Barr virus-induced lymphoma in allogeneic transplant recipients. *Blood* **92**, 1549–1555.

Saridakis, V., Sheng, Y., Sarkari, F., Holowaty, M. N., Shire, K., Nguyen, T., Zhang, R. G., Liao, J., Lee, W. & other authors (2005). Structure of the p53 binding domain of HAUSP/USP7 bound to Epstein–Barr nuclear antigen 1 implications for EBV-mediated immortalization. *Mol Cell* **18**, 25–36.

Savoldo, B., Huls, M. H., Liu, Z., Okamura, T., Volk, H. D., Reinke, P., Sabat, R., Babel, N., Jones, J. F. & other authors (2002). Autologous Epstein–Barr virus (EBV)-specific cytotoxic T cells for the treatment of persistent active EBV infection. *Blood* **100**, 4059–4066.

Straathof, K. C., Leen, A. M., Buza, E. L., Taylor, G., Huls, M. H., Heslop, H. E., Rooney, C. M. & Bollard, C. M. (2005). Characterization of latent membrane protein 2 specificity in CTL lines from patients with EBV-positive nasopharyngeal carcinoma and lymphoma. *J Immunol* **175**, 4137–4147.

Straus, S. E. (1988). The chronic mononucleosis syndrome. *J Infect Dis* **157**, 405–412.

Sugaya, N., Kimura, H., Hara, S., Hoshino, Y., Kojima, S., Morishima, T., Tsurumi, T. & Kuzushima, K. (2004). Quantitative analysis of Epstein–Barr virus (EBV)-specific $CD8^+$ T cells in patients with chronic active EBV infection. *J Infect Dis* **190**, 985–988.

Taketani, T., Kikuchi, A., Inatomi, J., Hanada, R., Kawaguchi, H., Ida, K., Oh-Ishi, T., Arai, T., Kishimoto, H. & Yamamoto, K. (2002). Chronic active Epstein–Barr virus infection (CAEBV) successfully treated with allogeneic peripheral blood stem cell transplantation. *Bone Marrow Transplant* **29**, 531–533.

Tao, Q., Robertson, K. D., Manns, A., Hildesheim, A. & Ambinder, R. F. (1998). Epstein–Barr virus (EBV) in endemic Burkitt's lymphoma: molecular analysis of primary tumor tissue. *Blood* **91**, 1373–1381.

Thorley-Lawson, D. A. & Gross, A. (2004). Persistence of the Epstein–Barr virus and the origins of associated lymphomas. *N Engl J Med* **350**, 1328–1337.

Tosato, G., Straus, S., Henle, W., Pike, S. E. & Blaese, R. M. (1985). Characteristic T cell dysfunction in patients with chronic active Epstein–Barr virus infection (chronic infectious mononucleosis). *J Immunol* **134**, 3082–3088.

Tsang, N. M., Chuang, C. C., Tseng, C. K., Hao, S. P., Kuo, T. T., Lin, C. Y. & Pai, P. C. (2003). Presence of the latent membrane protein 1 gene in nasopharyngeal swabs from patients with mucosal recurrent nasopharyngeal carcinoma. *Cancer* **98**, 2385–2392.

Tsuge, I., Morishima, T., Morita, M., Kimura, H., Kuzushima, K. & Matsuoka, H. (1999). Characterization of Epstein–Barr virus (EBV)-infected natural killer (NK) cell proliferation in patients with severe mosquito allergy; establishment of an IL-2-dependent NK-like cell line. *Clin Exp Immunol* **115**, 385–392.

Weinberger, B., Plentz, A., Weinberger, K. M., Hahn, J., Holler, E. & Jilg, W. (2004). Quantitation of Epstein–Barr virus mRNA using reverse transcription and real-time PCR. *J Med Virol* **74**, 612–618.

Williams, H. & Crawford, D. H. (2006). Epstein–Barr virus: the impact of scientific advances on clinical practice. *Blood* **107**, 862–869.

Young, L., Alfieri, C., Hennessy, K., Evans, H., O'Hara, C., Anderson, K. C., Ritz, J., Shapiro, R. S., Rickinson, A. & other authors (1989). Expression of Epstein–Barr virus transformation-associated genes in tissues of patients with EBV lymphoproliferative disease. *N Engl J Med* **321**, 1080–1085.

Zhang, Y., Nagata, H., Ikeuchi, T., Mukai, H., Oyoshi, M. K., Demachi, A., Morio, T., Wakiguchi, H., Kimura, N. & other authors (2003). Common cytological and cytogenetic features of Epstein–Barr virus (EBV)-positive natural killer (NK) cells and cell lines derived from patients with nasal T/NK-cell lymphomas, chronic active EBV infection and hydroa vacciniforme-like eruptions. *Br J Haematol* **121**, 805–814.

of a prospective randomized trial of the German Low Grade Lymphoma Study Group (GLSG). *Journal of Clinical Oncology*, **23,** 1984–1992.

Orciuolo, E., Buda, G., Cecconi, N., Galimberti, S., Versari, D., Cervetti, G., Salvetti, A. & Petrini, M. (2007) Unexpected cardiotoxicity in haematological bortezomib treated patients. *British Journal of Haematology*, **138,** 396–397.

Orlowski, R.Z., Nagler, A., Sonneveld, P., Blade, J., Hajek, R., Spencer, A., San Miguel, J., Robak, T., Dmoszynska, A., Horvath, N., Spicka, I., Sutherland, H.J., Suvorov, A.N., Zhuang, S.H., Parekh, T., Xiu, L., Yuan, Z., Rackoff, W. & Harousseau, J.L. (2007) Randomized phase III study of pegylated liposomal doxorubicin plus bortezomib compared with bortezomib alone in relapsed or refractory multiple myeloma: combination therapy improves time to progression. *Journal of Clinical Oncology*, **25,** 3892–3901.

Sonneveld, P., Hajek, R., Nagler, A., Spencer, A., Blade, J., Robak, T., Zhuang, S.H., Harousseau, J.L. & Orlowski, R.Z. (2008) Combined pegylated liposomal doxorubicin and bortezomib is highly effective in patients with recurrent or refractory multiple myeloma who received prior thalidomide/lenalidomide therapy. *Cancer*, **112,** 1529–1537.

Keywords: bortezomib, fludarabine, liposomal doxorubicin, mantle cell lymphoma, rituximab.

First published online 16 November 2009
doi: 10.1111/j.1365-2141.2009.07998.x

Serum granulysin as a possible biomarker of natural killer cell neoplasms

Granulysin is a cytolytic and proinflammatory molecule that is excreted from cytotoxic T lymphocytes (CTL) and natural killer (NK) cells. It is synthesized as a 15-kDa molecule and then cleaved at the amino and carboxy termini to produce an active 9-kDa form (Pena *et al*, 1997). Equivalent amounts of these two forms of granulysin are found in CTL and NK cells. However, the 9-kDa form is sequestered in cytolytic granules, while the 15-kDa form is constitutively secreted and more stable than the 9-kDa form when excreted *in vivo*. Therefore, the 15-kDa form constitutes a major portion of serum granulysin (Ogawa *et al*, 2003) and is considered to be a biomarker.

We have previously reported that serum granulysin reflects on cellular immune capacity (Ogawa *et al*, 2003), anti-tumour activity (Nagasawa *et al*, 2005) and graft-*versus*-host reaction in allogeneic transplantation (Nagasawa *et al*, 2006). Recently, it has been reported that granulysin is an important mediator of keratinocyte death in Stevens–Johnson syndrome and toxic epidermal necrolysis (Chung *et al*, 2008). Considering that granulysin is usually expressed in activated CTL, but not in resting or naive CTL, and constitutively expressed in NK cells, it was speculated that serum granulysin could be a biomarker for NK cell-related disease.

In this context, serum granulysin was retrospectively investigated in a patient with long-term NK type chronic active Epstein–Barr virus (EBV) infection (CAEBV). Serum granulysin was measured using our previously reported enzyme-linked immunosorbent assay method (Ogawa *et al*, 2003).

The patient presented with hydroa vacciniforme at the age of 8 years, and was diagnosed as NK type CAEBV when aged 9 years. In addition to the aggravation of facial skin lesion, general malaise progressed gradually. She was referred to our hospital at 16 years of age, and infusion of autologous activated T cells was started as a cell therapy. As no improvement was achieved, cytotoxic chemotherapy was started to eradicate EBV-infected cells. Although EBV load was markedly reduced after chemotherapy, the skin lesion did not improve and biopsy revealed the presence of EBV-infected cells (Fig 1B).

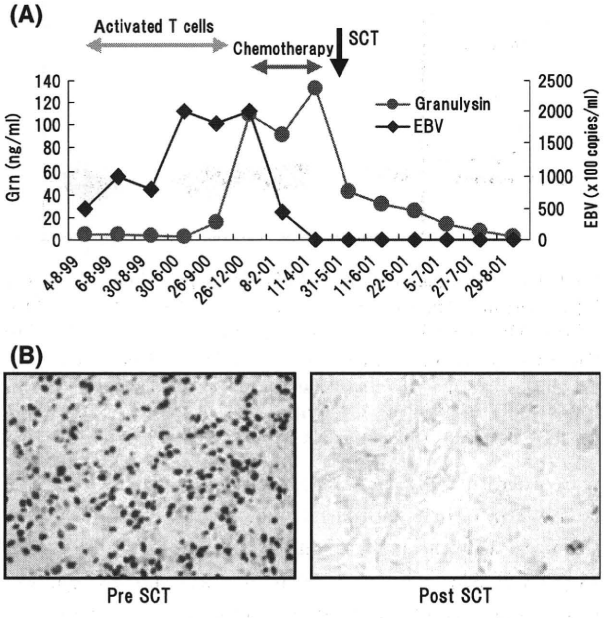

Fig 1. (A) Serum granulysin levels (Grn) and EBV genome load in the peripheral blood in a patient with NK type CAEBV. (B) EBV-infected cells in facial skin disappeared after SCT. EBER positive cells are stained dark brown. Original magnification ×400.

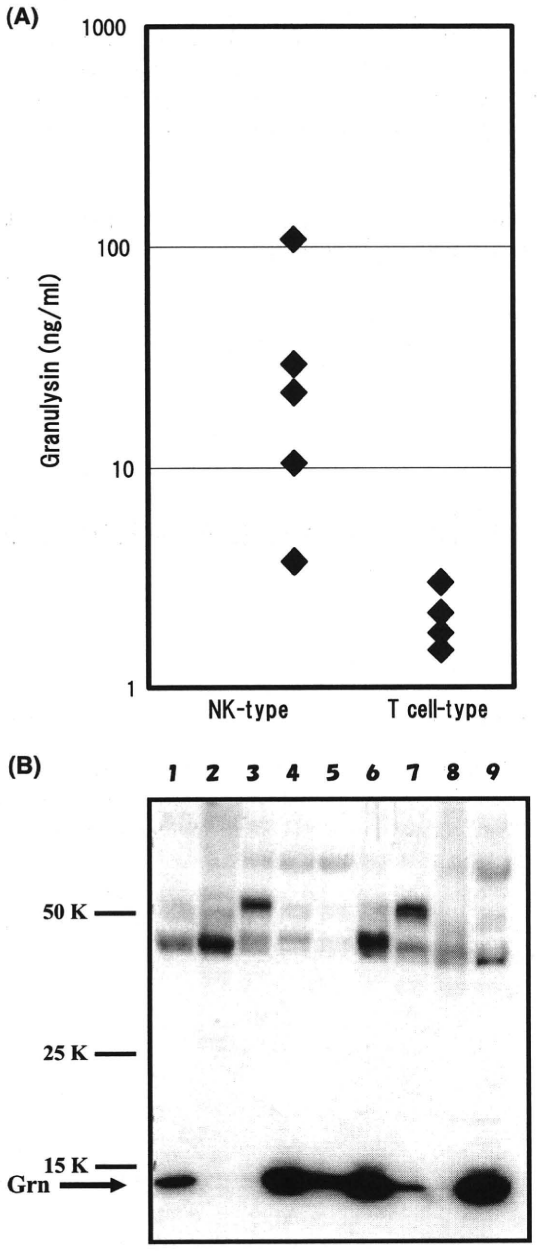

Fig 2. (A) Serum granulysin levels in five NK-type and four T cell-type (αβT) patients with CAEBV. (B) Expression of granulysin in EBV infected NK and γδ T cell lines. The monoclonal antibody, RF10 (Ogawa *et al*, 2003), which reacts with 15-kDa but not 9-kDa granulysin, was used for Western blotting. Lane number and cell line; 1:SNK1(NK) 2:SNK6(NK) 3:SNK8(γδT) 4:SNK10(NK) 5:SNK11(NK) 6:SNK5(NK) 7:SNK15(γδT) 8:SNK16(γδT) 9:SNK20(γδT).

In order to totally cure this condition, the patient received a bone marrow stem cell transplantation (SCT) from a human leucocyte antigen-identical unrelated donor at the age of 18 years. A skin biopsy performed after SCT showed complete disappearance of EBVinfected cells, and serum granulysin was reduced to levels within the normal range (1·5 ± 3·0 ng/ml; Fig 1A) (Ogawa *et al*, 2003).

We also investigated serum granulysin levels in patients with NK type and T cell-type (αβT cell) CAEBV (Kimura *et al*, 2005). Serum granulysin was elevated in NK type but not in T cell-type CAEBV (Fig 2A). Interestingly, serum granulysin was significantly elevated in one patient whose γδ T cells were infected with EBV (data not shown). Next, we investigated the expression of granulysin in several EBV-infected cell lines that were established from CAEBV patients. As expected, most of the NK and γδ T cell lines expressed granulysin (Fig 2B). (SNK11 clone was established from the patient described above and it was clonal in terms of EBV infection). Interestingly, tumour necrosis factor α (TNF-α) was exclusively excreted from the granulysin-expressing cell lines, although interferon-γ was produced in all cell lines (data not shown). From these observations, serum granulysin seems to be a useful biomarker of NK cell neoplasms and could be a marker of its malignant transformation, although the NK proliferative diseases examined here were all EBV-related. Comparison between EBV- and non-EBV- related NK or γδT cell disorders is also an interesting issue regarding not only their pathophysiology but also the mechanism of granulysin regulation, which is not precisely known yet. Further investigation is required to determine its clinical use and significance.

Masayuki Nagasawa[1]
Kazuyuki Ogawa[2]
Kinya Nagata[2]
Norio Shimizu[3]

[1]*Department of Developmental Biology, Tokyo Medical and Dental University, Post Graduate School, Tokyo,* [2]*B.M.L. R&D Centre, Saitama, and* [3]*Department of Virology, Tokyo Medical and Dental University, Post Graduate School, Tokyo, Japan.*
E-mail: mnagasawa.ped@tmd.ac.jp

References

Chung, W.H., Hung, S.I., Yang, J.Y., Su, S.C., Huang, S.P., Wei, C.Y., Chin, S.W., Chiou, C.C., Chu, S.C., Ho, H.C., Yang, C.H., Lu, C.F., Wu, J.Y., Liao, Y.D. & Chen, Y.T. (2008) Granulysin is a key mediator for disseminated keratinocyte death in Stevens–Johnson syndrome and toxic epidermal necrolysis. *Nature Medicine*, **12,** 1343–1350.

Kimura, H., Hoshino, Y., Hara, S., Sugaya, N., Kawada, J., Shibata, Y., Kojima, S., Nagasaka, T., Kuzushima, K. & Morishima, T. (2005) Differences between T cell-type and natural killer cell-type chronic active Epstein–Barr virus infection. *The Journal of Infectious Disease*, **191,** 531–539.

Nagasawa, M., Kawamoto, H., Tsuji, Y. & Mizutani, S. (2005) Transient increase of serum granulysin in stage IVs neuroblastoma patient during spontaneous regression: case report. *International Journal of Hematology*, **82,** 456–457.

Nagasawa, M., Isoda, T., Itoh, S., Kajiwara, M., Morio, T., Shimizu, N., Ogawa, K., Nagata, K., Nakamura, M. & Mizutani, S. (2006) Analysis of serum granulysin in patients with hematopoietic stem cell transplantation: its usefulness as a marker of graft-versus-host reaction. *American Journal of Hematology*, **81,** 340–348.

Ogawa, K., Takamori, Y., Suzuki, K., Nagasawa, M., Takano, S., Kasahara, Y., Nakamura, Y., Kondo, S., Sugamura, K., Nakamura, M. & Nagata, K. (2003) Granulysin in human serum as a marker of cell-mediated immunity. *European Journal of Immunology*, **33,** 1925–1933.

Pena, S.V., Hanson, D.A., Carr, B.A., Goralski, T.J. & Krensky, A.M. (1997) Processing, subcellular localization, and function of 519 (granulysin), a human late T cell activation molecule with homology to small, lytic, granule proteins. *Journal of Immunology*, **158,** 2680–2688.

Keywords: granulysin, natural killer cells, chronic active EBV infection, γδ T cells.

First published online 13 November 2009
doi: 10.1111/j.1365-2141.2009.07999.x

THE JOURNAL OF BIOLOGICAL CHEMISTRY VOL. 285, NO. 41, pp. 31774–31782, October 8, 2010

BCR-ABL but Not JAK2 V617F Inhibits Erythropoiesis through the Ras Signal by Inducing $p21^{CIP1/WAF1}$*[S]

Received for publication, February 28, 2010, and in revised form, July 24, 2010 Published, JBC Papers in Press, July 27, 2010, DOI 10.1074/jbc.M110.118653

Masahiro Tokunaga[‡], Sachiko Ezoe[‡§1], Hirokazu Tanaka[‡], Yusuke Satoh[‡], Kentaro Fukushima[‡], Keiko Matsui[‡], Masaru Shibata[‡], Akira Tanimura[‡], Kenji Oritani[‡], Itaru Matsumura[‡¶], and Yuzuru Kanakura[‡]

From the [‡]Department of Hematology and Oncology, Osaka University Graduate School of Medicine, 2-2 Yamada-oka, Suita, Osaka 565-0871, the [§]Medical Center of Translational Research, Osaka University Hospital, Suita, Osaka 565-0871, and the [¶]Division of Hematology, Department of Internal Medicine, Kinki University School of Medicine, Osaka-Sayama, Osaka 589-8511, Japan

BCR-ABL is a causative tyrosine kinase (TK) of chronic myelogenous leukemia (CML). In CML patients, although myeloid cells are remarkably proliferating, erythroid cells are rather decreased and anemia is commonly observed. This phenotype is quite different from that observed in polycythemia vera (PV) caused by JAK2 V617F, whereas both oncogenic TKs activate common downstream molecules at the level of hematopoietic stem cells (HSCs). To clarify this mechanism, we investigated the effects of BCR-ABL and JAK2 V617F on erythropoiesis. Enforced expression of BCR-ABL but not of JAK2 V617F in murine LSK (Lineage$^-$Sca-1^{hi}CD117^{hi}) cells inhibited the development of erythroid cells. Among several signaling molecules downstream of BCR-ABL, an active mutant of N-Ras (N-RasE12) but not of STAT5 or phosphatidylinositol 3-kinase (PI3-K) inhibited erythropoiesis, while N-RasE12 enhanced the development of myeloid cells. BCR-ABL activated Ras signal more intensely than JAK2 V617F, and inhibition of Ras by manumycin A, a farnesyltransferase inhibitor, ameliorated erythroid colony formation of CML cells. As for the mechanisms of Ras-induced suppression of erythropoiesis, we found that GATA-1, an erythroid-specific transcription factor, blocked Ras-mediated mitogenic signaling at the level of MEK through the direct interaction. Furthermore, enforced expression of N-RasE12 in LSK cells derived from p53-, $p16^{INK4a}$/$p19^{ARF}$-, and $p21^{CIP1/WAF1}$-null/wild-type mice revealed that suppressed erythroid cell growth by N-RasE12 was restored only by $p21^{CIP1/WAF1}$ deficiency, indicating that a cyclin-dependent kinase (CDK) inhibitor, $p21^{CIP1/WAF1}$, plays crucial roles in Ras-induced suppression of erythropoiesis. These data would, at least partly, explain why respective oncogenic TKs cause different disease phenotypes.

Oncogenic tyrosine kinases (TKs)[2] such as BCR-ABL, FLT3-ITD, and JAK2 V617F are known to confer growth and/or survival advantage on hematopoietic cells, thereby causing hematologic malignancies (1–3). These gene alterations are supposed to occur at the hematopoietic stem cell (HSC) level (3, 4). Although these oncogenic TKs activate common downstream pathways including Ras/Raf/MEK/ERK, PI3-K/Akt, and STAT (1, 2, 5), their disease phenotypes are quite different: BCR-ABL is a causative gene of chronic myelogenous leukemia (CML) (1), FLT3-ITD of acute myeloid leukemia (AML) (2), and JAK2 V617F of myeloproliferative neoplasms including polycythemia vera (PV), essential thrombocythemia (ET) and primary myelofibrosis (PMF) (3). In patients with chronic-phase CML, anemia is a common feature in contrast to the marked leukocytosis in the peripheral blood. Also, bone marrow (BM) examination shows that erythroid islands are reduced in number and size despite the increased cellularity due to the granulocytic proliferation (6). This disease phenotype is totally different from that of PV, in which JAK2 V617F causes erythrocytosis together with the mild leukocytosis and thrombocytosis. Furthermore, in blast-phase CML, blast lineages are generally myeloid or lymphoid, and erythroid crisis is a rare incidence with a frequency no more than 5% (7, 8). These data suggest that, in contrast to the trilinear promoting activities of JAK2 V617F, BCR-ABL might not support the development of erythroid cells.

BCR-ABL activates several downstream pathways including Ras/Raf/MEK/ERK, STAT5, and PI3-K/Akt pathways (1, 4). Among them, we have previously shown that Ras plays crucial roles in the growth and survival of BCR-ABL-positive K562 cells, while STAT5 and PI3-K pathways contribute to their growth and survival to the only limited extent (9). In addition, although the role of STAT5 in BCR-ABL-mediated leukemogenesis remains controversial (10, 11), another group also reported that transformation of murine BM cells by BCR-ABL is blocked by dominant-negative Ras (12). Furthermore, Ras signaling was shown to be indispensable for the pathogenesis of CML in a murine BM transplantation model (13). Therefore, the activated Ras is considered to be essential for the pathogenesis of CML, and is also speculated to principally determine the disease phenotype of CML, that is, prominent proliferation of myeloid cells accompanied by the suppressed erythropoiesis.

* This work was supported by grants from the Ministry of Education, Science, Sports, and Culture and Technology of Japan.

[S] The on-line version of this article (available at http://www.jbc.org) contains supplemental Table S1 and Methods.

[1] To whom correspondence should be addressed. Tel.: 81-6-6879-3871; Fax: 81-6-6879-3879; E-mail: sezoe@bldon.med.osaka-u.ac.jp.

[2] The abbreviations used are: TK, tyrosine kinase; CML, chronic myelogenous leukemia; PV, polycythemia vera; HSC, hematopoietic stem cell; LSK, Lineage$^-$Sca-1^{hi}CD117^{hi}; BM, bone marrow; CDK, cyclin-dependent kinase; rh, recombinant human; TPO, thrombopoietin; rm, recombinant murine; EPO, erythropoietin; SCF, stem cell factor; G1ERT, GATA-1/ERT; 4-HT, 4-hydroxytamoxifen; Ab, antibody; HPRT, hypoxanthine phosphoribosyl transferase; pRb, retinoblastoma protein; PRAK, p38-regulated/activated protein kinase.

Ras is constitutively activated by various oncogenic TKs or mutations of Ras itself in various malignant tumors. Although oncogenic (or constitutively activated) Ras was originally shown to transmit mitogenic and survival signals through Raf/MEK/ERK (14), recent studies have demonstrated that, like other oncogenic stimuli, it also induces growth inhibition/arrest in normal cells to prevent their malignant transformation. In general, this biological phenomenon is called "cellular senescence" and observed in various types of non-hematopoietic cells (15, 16). In addition, excessive Ras signaling was reported to inhibit erythropoiesis (17, 18), indicating the presence of a similar cellular response in hematopoietic cells. So far, oncogenic Ras has been shown to cause senescence through several signaling pathways other than Raf/MEK/ERK (15, 19–21). Also, several cell cycle regulatory molecules such as p53, p16^{INK4a}, p19^{ARF} and p21$^{CIP1/WAF1}$, have been shown to play central roles in oncogene-induced senescence (15, 19, 21).

In this report, we found that BCR-ABL but not JAK2 V617F, and among their downstream molecules, Ras but not STAT5 or PI3-K suppress erythropoiesis from murine LSK cells. As for this mechanism, we found that an erythroid-lineage specific transcription factor, GATA-1, blocks Ras-dependent growth and survival by inhibiting MEK1 activity through the direct interaction. Furthermore, we showed that a cyclin-dependent kinase (CDK) inhibitor, p21$^{CIP1/WAF1}$, plays crucial roles in Ras-induced suppression of erythropoiesis using p21$^{CIP1/WAF1}$-deficient hematopoietic cells.

EXPERIMENTAL PROCEDURES

Cytokines and Reagents—Recombinant human thrombopoietin (rhTPO) and recombinant murine interleukin-3 (rmIL-3) were provided by Kyowa Hakko Kirin (Tokyo, Japan). Recombinant human erythropoietin (rhEPO) and murine stem cell factor (rmSCF) were purchased from R & D Systems (Minneapolis, MN). Manumycin A was purchased from Merck KGaA (Darmstadt, Germany).

Plasmid Constructs and cDNAs—Expression vectors for GATA-1/ERT (G1ERT) and wild-type (WT) GATA-1 were described previously (22). Active forms of N-Ras (N-RasE12) (23) and STAT5A (1*6 STAT5A) (24), and membrane-targeted PI3-K catalytic subunit (p110^{CAAX}) (25) were subcloned into pMYs-IRES-EGFP, a retrovirus expression vector, which was kindly provided by Dr. T. Kitamura (University of Tokyo, Tokyo, Japan). pMSCV-IRES-GFP-p210-BCR-ABL is a generous gift from Dr. C. J. Eaves (Terry Fox Laboratory, Vancouver, BC, Canada) (26). The cDNA of JAK2 V617F was kindly provided by Dr. K. Shimoda (University of Miyazaki, Miyazaki, Japan) (27) and was subcloned into pMSCV-IRES-GFP.

Cell Lines and Cultures—A murine IL-3-dependent hematopoietic cell line, Ba/F3, was maintained in RPMI (nacalai tesque, Kyoto, Japan) supplemented with 10% fetal bovine serum (FBS) (Equitech-Bio, Kerrville, TX) and 0.3 ng/ml rmIL-3. NIH3T3 and 293T cells were cultured in Dulbecco's modified Eagle's medium (DMEM; nacalai tesque) supplemented with 10% FBS.

Preparation of Stable Transformants from Ba/F3—We introduced G1ERT into Ba/F3 cells by electroporation (250 V and 950 microfarads) and selected stably transfected clones by the culture with G-418 (1.0 mg/ml; Wako Pure Chemical Industries, Osaka, Japan). We further introduced pMYs-IRES-EGFP-N-RasE12 and obtained doubly transfected clones by sorting GFP-positive cells with BD FACSAria Cell-Sorting System (BD Biosciences, San Jose, CA). Their IL-3-independent growth and cell cycle were analyzed with or without the activation of GATA-1 by 4-hydroxytamoxifen (4-HT; Sigma-Aldrich). DNA contents of the cells were evaluated by staining with propidium iodide.

Luciferase Assays—Luciferase assays were performed with a Dual-Luciferase Reporter Assay System (Promega, Madison, WI) as previously described (22). As for assays using Ba/F3 cells, transfection was performed with Amaxa Nucleofector technology (Lonza, Cologne, Germany), followed by the measurement of luciferase activities after 24 h.

Immunoblotting and Coimmunoprecipitation Analyses—Preparation of cell lysates, immunoprecipitation, gel electrophoresis, and immunoblotting were performed according to the methods described previously (22, 28). Antibodies (Abs) and reagents were supplied by the manufacturers described in supplemental methods.

Glutathione S-transferase (GST) Pull-down Assays—GST pull-down assays were performed as previously reported (22).

Animals—The congenic C57BL/6J mice were purchased from Clea Japan, Inc. (Tokyo, Japan). B6.129-Cdkn2a^{tm1Rdp} (p16^{INK4a}/p19^{ARF}-null) mice and p53-null mice were kindly provided by Technology Transfer Center National Cancer Institute (Rockville, MD) and Dr. N. Nishimoto (Wakayama Medical University, Wakayama, Japan), respectively. B6.129S2-Cdkn1a^{tm1Tyj}/J (p21$^{CIP1/WAF1}$-null) mice were purchased from The Jackson Laboratory (Bar Harbor, ME). The experimental designs of this study were approved by the Institutional Animal Care and Use Committee at Osaka University Graduate School of Medicine.

Separation of Murine Hematopoietic Progenitors—Murine BM cells were flushed from both femora and tibiae, and progenitors were concentrated by anti-mouse CD117 MicroBeads and autoMACS Pro Separator (Miltenyi Biotec, Bergisch Gladbach, Germany). To isolate LSK (Lineage$^-$Sca-1^{hi}CD117^{hi}) cells, selected progenitors were stained with phycoerythrin-conjugated (PE-conjugated) monoclonal Abs against murine lineage markers (CD3e (145–2C11), CD45R/B220 (RA3–6B2), Gr-1 (RB6–8C5), CD11b (M1/70), and TER-119 (TER-119)), fluorescein isothiocyanate-conjugated (FITC-conjugated) anti-Sca-1 Ab (E13–161.7), and allophycocyanin-conjugated (APC-conjugated) anti-CD117 Ab (2B8), and isolated by FACSAria. All Abs were purchased from BD Biosciences.

Preparation of Retrovirus Particles—Preparation of retrovirus particles was performed as described previously (29) (see supplemental methods).

Retrovirus Transfection into Murine BM Progenitors—Isolated LSK cells were precultured overnight in DMEM supplemented with 10% FBS, rmSCF (100 ng/ml), and rhTPO (100 ng/ml). Then, the cells were seeded on 24-well tissue plates coated with RetroNectin (TaKaRa Bio Inc., Shiga, Japan), infected with each viral supernatant by spinoculation, and cultured in the same medium containing 10% FBS, protamine sulfate (10 μg/ml; Sigma-Aldrich), rmSCF (50 ng/ml), and rhTPO (50 ng/ml). After 48 h of culture, retrovirus-transduced GFP$^+$

cells were sorted with FACSAria and were subjected to colony assays or stromal coculture.

Colony Assays—Cells were plated at the indicated density in methylcellulose medium (MethoCult; Stem Cell Technologies, Vancouver, BC, Canada) supplemented with the indicated growth factors. Cells were incubated with 5% CO_2 at 37 °C, and the numbers of colonies were counted after the indicated days.

Stromal Coculture—A murine BM stromal cell line, MS-5, was cultured in minimum essential medium (MEM) α (Invitrogen, Carlsbad, CA) with 10% FBS and prepared in 24-well tissue plates 1 day before the seeding. The sorted GFP$^+$ progenitors were seeded (1.5×10^3 cells/well) on the monolayer of MS-5 and cocultured in 2 ml of MEMα supplemented with 10% FBS, rmSCF (50 ng/ml), and rhEPO (3 units/ml). Five days after the initiation of coculture, hematopoietic cells were harvested and stained with PE-conjugated anti-CD45 (30-F11) Ab, and APC-conjugated anti-CD11b (M1/70) or anti-TER-119 (TER-119) Ab (all of them from BD Biosciences). To evaluate the phosphorylation status of ERK1/2, we used BD Phosflow technology (BD Biosciences). The harvested cells were further incubated in DMEM containing 2% FBS without cytokines for 4 h, then fixed, permeabilized, and stained with Alexa Fluor®647-conjugated anti-ERK1/2 (pT202/pY204) Ab (BD Biosciences) according to the manufacturer's recommendation.

Flow Cytometric Analyses—Flow cytometric analyses were performed using BD FACSCanto II (BD Biosciences). The data analyses were done with BD FACSDiva software (BD Biosciences) or FlowJo software (TreeStar, Ashland, OR).

Immunofluorescence Microscopy—5×10^4 of the transduced cells were cytospun onto microscope slides, fixed in 2% paraformaldehyde, and permeabilized in 1% Nonidet P-40 in PBS. After the incubation in blocking buffer (1 mg/ml of γ-globulin in PBS), the slides were incubated with a monoclonal Ab against p16^{INK4a} (F-12) or p19^{ARF} (5-C3–1) (both from Santa Cruz Biotechnology, Santa Cruz, CA). The slides were then incubated with an Alexa Fluor®546-conjugated secondary antibody (goat anti-mouse IgG for p16^{INK4a}, or goat anti-rat IgG for p19^{ARF}), followed by the staining of nuclei with Hoechst 33342 (all from Invitrogen). The slides were mounted in Fluoromount (Diagnostic BioSystems, Pleasanton, CA) before viewing on a LSM 5 PASCAL microscope (Carl Zeiss, Oberkochen, Germany).

Semiquantitative RT-PCR—Total RNA was isolated from 5×10^3 of the transduced cells using RNeasy Mini Kit (Qiagen, Hilden, Germany) and converted to cDNA by SuperScript III First Strand Synthesis System (Invitrogen). PCR was performed using Ampli Taq Gold (Applied Biosystems, Carlsbad, CA) with primers described in supplemental Table S1.

Real-time RT-PCR—Quantitative real-time RT-PCR was performed using FastStart Universal SYBR Green Master (Roche Diagnostics GmbH, Mannheim, Germany) and PRISM 7900HT (Applied Biosystems). Amplified signals were normalized to the levels of hypoxanthine phosphoribosyl transferase (HPRT). The primer sequences are described in supplemental Table S1.

BM Samples from CML Patients—BM samples were obtained from three patients with newly diagnosed chronic-phase CML. CD34$^+$ cells were separated using the MACS immunomagnetic separation system, and were subjected to colony assays. All BM samples were obtained after receiving written informed consent in accordance with the Declaration of Helsinki, and this study protocol was approved by the institutional review board of Osaka University Hospital.

Statistical Methods—Statistical analyses were carried out by standard Student *t* tests. Error bars used throughout indicate S.D.

RESULTS

BCR-ABL but Not JAK2 V617F Inhibits the Development of Erythroid Cells—To examine the effects of BCR-ABL on erythropoiesis, we first introduced p210-BCR-ABL into murine LSK cells using the retrovirus vector harboring GFP as a reporter gene. After 48 h, GFP$^+$ cells were sorted and cocultured with a murine BM stromal cell line, MS-5, in the presence of rmSCF and rhEPO for 5 days. As compared with mock-transduced cells, the proportion of CD45^{low}TER-119$^+$ erythroid cells was reduced in BCR-ABL-transduced cells significantly (Fig. 1*A*). We also examined the effects of JAK2 V617F on erythropoiesis with the same strategy and found that JAK2 V617F did not reduce the proportion of erythoroid cells. In colony assays, BCR-ABL significantly decreased the number of burst-forming units-erythroid (BFU-E), while it increased the number of myeloid colonies (Fig. 1*B*). On the other hand, JAK2 V617F did not reduce the number of BFU-E. These data indicate that BCR-ABL but not JAK2 V617F inhibits the development of erythroid cells from murine hematopoietic progenitors.

Oncogenic Ras Inhibits Erythropoiesis Downstream of BCR-ABL—BCR-ABL activates mainly Ras/Raf/MEK/ERK, JAK2/STAT5, and PI3-K/Akt pathways. Next, to examine the roles of these pathways in erythropoiesis, we transduced LSK cells with an active form of each signal transduction molecule: N-RasE12 for an active form of N-Ras, 1*6 STAT5A for STAT5, and p110^{CAAX} for PI3-K. Compared with Mock, 1*6 STAT5A and p110^{CAAX} increased total erythroid cell numbers by 2.8- and 1.9-fold, respectively (both, $p < 0.05$), while the proportion of erythroid cells was scarcely influenced by both molecules due to the increase in total cell numbers (Fig. 2, *A* and *B*). In contrast, N-RasE12 remarkably reduced not only the frequency (Fig. 2*A*) but also the number of erythroid cells (0.28-fold) (Fig. 2*B*), while it significantly increased the number of CD11b$^+$-myeloid cells (Fig. 2*C*). We also performed colony assays using N-RasE12- or Mock-transduced LSK cells. As shown in Fig. 2*D*, N-RasE12 significantly reduced the number of BFU-E (average colony numbers from 1.0×10^3 cells input: Mock-transduced cells, 9.7; N-Ras-transduced cells, 0.33) ($p < 0.01$).

BCR-ABL Activates Ras Signal More Intensely than JAK2 V617F—Next, we tried to clarify why JAK2 V617F did not suppress erythropoiesis, because it has been reported to activate Ras as well as BCR-ABL (5). For this purpose, we introduced JAK2 V617F and BCR-ABL into murine LSK cells, cocultured them with MS-5, and evaluated the Ras activity by expediently measuring the phosphorylation status of ERK1/2 after 4-h starvation of cytokines. As shown in Fig. 2*E*, ERK1/2 was more intensely phosphorylated (activated) in cells transduced with BCR-ABL than in those with JAK2 V617F. We also examined the phosphorylation status of ERK1/2 in CML patients' blood

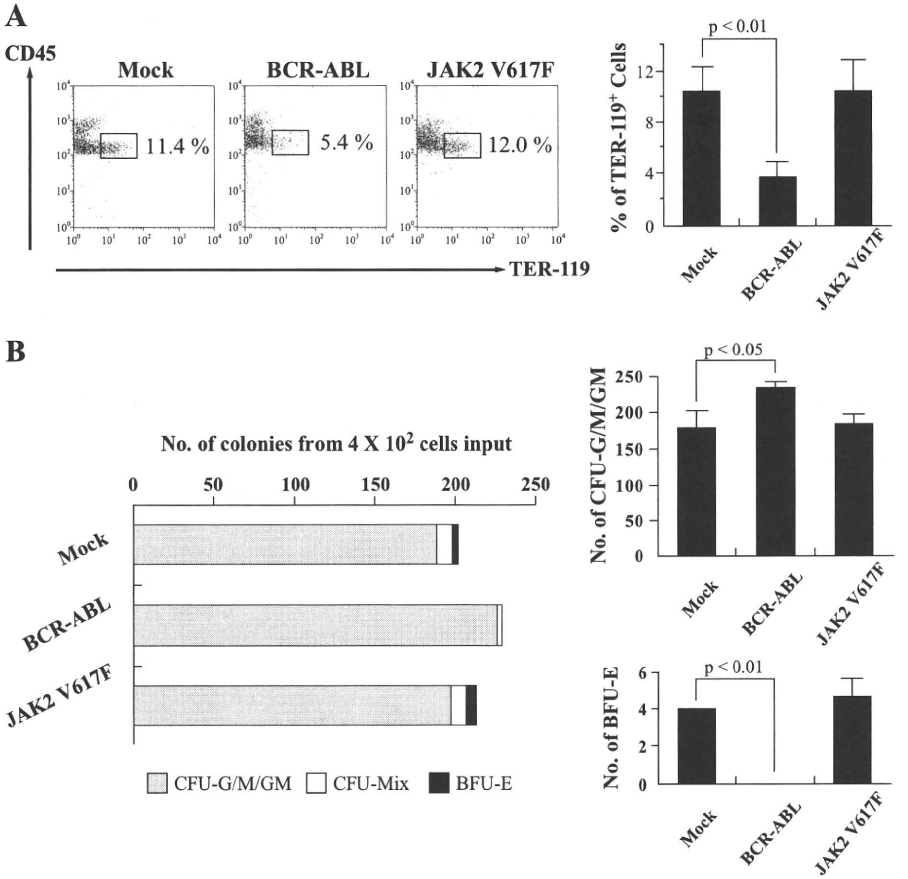

FIGURE 1. **Effects of oncogenic TKs on proliferation of erythroid cells.** *A*, after infection of retrovirus expressing Mock, BCR-ABL, or JAK2 V617F into murine LSK cells, GFP$^+$ cells were sorted and cocultured with MS-5 in the presence of rmSCF and rhEPO. After 5-day cultures, expression of CD45 and TER-119 was analyzed by flow cytometry (*left panels*). The proportions of CD45^{low}TER-119$^+$ cells are shown in the *right bar graph* ($n = 3$). *B*, respective retrovirus-transduced LSK cells were seeded at a density of 2.0×10^2 cells/35-mm dish in methylcellulose medium containing rmSCF, rmIL-3, rmIL-6, rhTPO, and rhEPO. Colony numbers were counted after 9 days. Representative colony numbers (*left*) and myeloid/erythroid colony numbers (*right*, $n = 3$) are shown. BFU-E, burst-forming units-erythroid; CFU-G/M/GM, colony-forming unit-granulocyte/macrophage/granulocyte-macrophage.

cells treated with manumycin A, a potent farnesyltransferase inhibitor which selectively suppresses Ras, or vehicle only. As shown in Fig. 2*F*, phosphorylation of ERK was reduced by Ras inhibition, indicating that BCR-ABL activates ERK through the activation of Ras. These data indicate that different growth status of erythroid cells between these TKs might result from the preferential activation of Ras signal by BCR-ABL.

Suppression of Ras Signal Ameliorates the Inhibition of Erythropoiesis Caused by BCR-ABL—Furthermore, to make sure that suppressed erythropoiesis caused by BCR-ABL is due to the activation of Ras signal, we examined the effects of Ras-inhibition on erythroid colony formation of BCR-ABL expressing cells. CD34$^+$ cells were separated from BM samples of three patients with newly diagnosed chronic-phase CML. They were then cultured in methylcellulose medium containing rhSCF, rhIL-3, and rhEPO, with or without manumycin A. Complete blockage of Ras signal by supplement of sufficient dose (10 μM) of manumycin A eradicated erythroid colony formation (data not shown). However, as shown in Fig. 2*G*, the number of erythroid colonies was restored by low doses of manumycin A in all three patients, though there was some difference in degree. This result, actually in primary CML cells, supports our model that, although Ras is indispensable for erythroid cell survival, excessive Ras signal downstream of BCR-ABL rather inhibits erythroid cell proliferation.

GATA-1 Inhibits Ras-dependent Cell Proliferation and Survival—As described above, oncogenic Ras signaling promoted the proliferation of myeloid cells, but inhibited that of erythroid cells. To elucidate the mechanisms underlying the different responses to oncogenic Ras between the two lineages, we examined the effects of GATA-1, which is expressed in erythroid cells but not in myeloid cells, on Ras signal. For this purpose, we transduced N-RasE12 and G1ERT, a chimera gene consisting of full-length GATA-1 and the mutated ligand-binding domain of estrogen receptor, into Ba/F3 cells, which was named Ba/F3/N-RasE12/G1ERT. G1ERT reveals GATA-1 activity in response to 4-HT as previously reported (22). As shown in Fig. 3*A*, N-RasE12 enabled this clone to proliferate and survive independently of IL-3. However, when GATA-1 activity was induced by 4-HT treatment, N-RasE12-dependent cell growth was completely suppressed (Fig. 3*A*). In agreement with this result, the proportion of growing cells in S-G2/M phase was reduced by 4-HT treatment from 36% to 8% in DNA contents analysis (Fig. 3*B*). Furthermore, 4-HT treatment induced apoptosis in 78% of cells, which was detected as a subdiploid fraction. From these results, we speculated that GATA-1 might inhibit oncogenic Ras activities, which transmit proliferation and survival signals.

GATA-1 Suppresses MEK Activity—Ras signal is known to be transmitted to the nucleus through Raf, MEK, and ERK in this order. To identify which molecule was inhibited by GATA-1 in this pathway, we performed luciferase assays using a reporter gene for ERK (3 × AP-1-Luc) in NIH3T3 and Ba/F3 cells. As shown in Fig. 4, *A* and *B*, GATA-1 significantly reduced the N-Ras- and MEK1-induced AP-1-luciferase activities almost to the baseline levels (*white boxes*), which indicates that GATA-1 inhibits Ras signal at the level or downstream of MEK. Next, we examined the phosphorylation status of MEK1/2 and ERK1/2 in Ba/F3/N-RasE12/G1ERT cells by immunoblot analysis. As shown in Fig. 4*C*, both MEK1/2 and ERK1/2 were phosphorylated by N-RasE12 even under the culture without IL-3, which was suppressed by 4-HT in a time-dependent manner. This

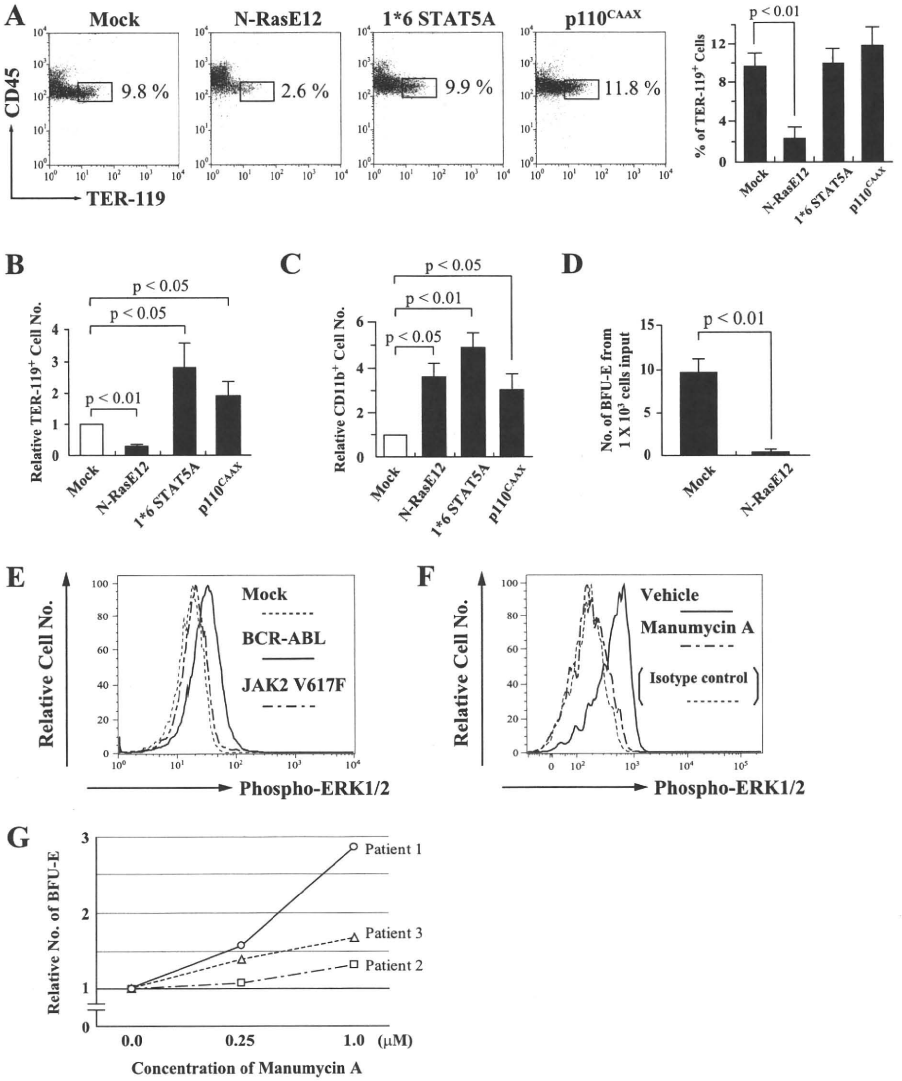

FIGURE 2. **Roles of downstream molecules of oncogenic TKs in erythropoiesis.** *A–C*, LSK cells each transfected with the indicated gene were cocultured with MS-5 in the medium containing rmSCF and rhEPO. After 5 days, expression of CD45 and TER-119 was analyzed by flow cytometry (*A*, *left panels*) and the proportions of CD45^{low}TER-119^{+} cells are shown (*A*, *right bar graph*, $n = 3$). Numbers of the TER-119^{+} cells were calculated by multiplication of the frequencies and total cell numbers. Relative numbers to Mock are shown (*B*). Relative CD11b^{+} myeloid cell numbers are shown (*C*). *D*, retrovirus-infected LSK cells were seeded at a density of 5.0×10^2 cells/dish in methylcellulose medium containing rmSCF, rmIL-3, and rhEPO. The numbers of BFU-E were counted after 8 days ($n = 3$). *E*, LSK cells, each transfected with Mock, BCR-ABL, or JAK2 V617F, were further incubated without cytokines after the coculture with MS-5, and the phosphorylation status of ERK1/2 was analyzed using Phosflow technology. *F*, after 5-h incubation of CML patients blood mononuclear cells with manumycin A (7 μM) or vehicle, the phosphorylation status of ERK1/2 was analyzed. *G*, CD34^{+} cells were separated from BM samples of three CML patients, and seeded in methylcellulose medium containing rhSCF, rhIL-3, and rhEPO, with manumycin A at the indicated concentrations or vehicle. The numbers of BFU-E were counted after 9 days, and shown as relative numbers to vehicle in each patient.

result implies that GATA-1 suppresses Ras signal at the level or upstream of MEK. Together with the results from luciferase assays, it was speculated that GATA-1 would inhibit MEK activity.

GATA-1 Blocks the Ras Signal through Its Direct Interaction with MEK1—To clarify how GATA-1 inhibits MEK activities, we examined the interaction between GATA-1 and MEK1. First, we transfected 293T cells with hemagglutinin-tagged (HA-tagged) GATA-1 and/or Flag-tagged MEK1. Total cellular lysates were prepared after 36 h, and GATA-1 was immunoprecipitated with the anti-HA Ab and MEK1 with the anti-Flag Ab. As shown in Fig. 4*D*, immunoblotting with the anti-Flag Ab showed that MEK1 was coimmunoprecipitated with GATA-1 only when both molecules were cotransduced. Also, immunoblotting with the anti-HA Ab showed that GATA-1 was coimmunoprecipitated with MEK1.

Next, to examine whether endogenous GATA-1 and MEK interact in primary erythroid cells, we performed a coimmunoprecipitation analysis using murine BM erythroid cells: Cells positive for CD71 (transferrin receptor), which is expressed at high levels on erythroid progenitors, were purified using the MACS immunomagnetic separation system. Total cellular lysate was prepared and subjected to immunoprecipitation with an anti-GATA-1 Ab or rat isotype IgG. Fig. 4*E* shows that MEK is coimmunoprecipitated with GATA-1, indicating that these molecules actually interact with each other in primary erythroid cells.

Finally, we investigated whether MEK1 directly binds to GATA-1 *in vitro* by GST pull-down assays. After verifying the quality and quantity of GST-MEK1 fusion protein by Coomassie Brilliant Blue staining (data not shown), we analyzed the binding between GST-MEK1 and *in vitro*-translated GATA-1. As shown in Fig. 4*F*, GST-MEK1 but not GST alone, bound to ^{35}S-labeled GATA-1 *in vitro*.

Together with the results of Fig. 4, *A–C*, we proved the following two facts: GATA-1 inhibits MEK activation; GATA-1 and MEK interact with each other in primary erythroid progenitors. From these facts, we speculated that GATA-1 blocks Ras signal at least partly through the direct interaction with MEK1.

Oncogenic Ras Induces Suppression of Erythropoiesis through the Induction of p21$^{CIP1/WAF1}$—In addition to the functions to deliver mitogenic and anti-apoptotic signals (14), Ras paradoxically causes growth arrest (senescence) in normal cells through several cell cycle regulatory molecules such as p53, p16^{INK4a}, p19^{ARF}, and p21$^{CIP1/WAF1}$ (15, 21). Among them, p53 is a tumor-suppressor and acts as a pivotal regulator of these responses (15, 16, 19, 21). p19^{ARF} is a splicing variant of p16^{INK4a} and inhibits the function of H/MDM2, which pro-

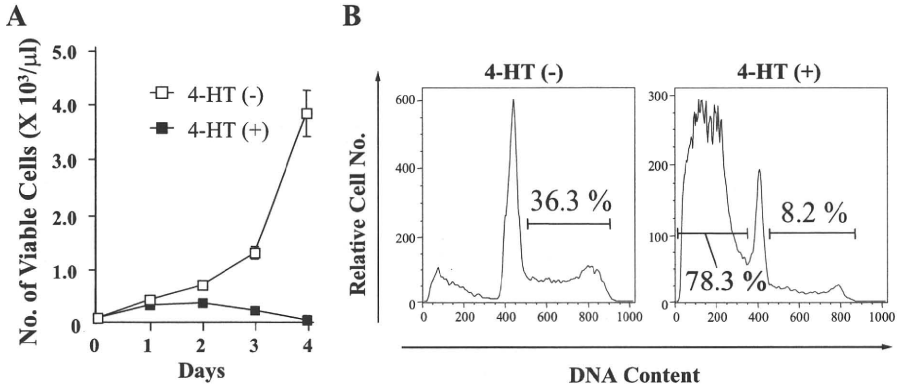

FIGURE 3. **Inhibition of Ras-dependent cell proliferation and survival by GATA-1.** *A*, Ba/F3/N-RasE12/G1ERT cells were seeded at a density of 100/μl and cultured in RPMI supplemented with 1% FBS without IL-3 in the presence or absence of 1 μM 4-HT. Total numbers of viable cells were counted by trypan blue dye exclusion method on the indicated days. The results are shown as means ± S.D. of triplicate cultures. *B*, after 48 h of culture, DNA contents of 4-HT-treated or untreated cells were examined by propidium iodide staining. The proportions of cells in S-G2/M phase and subdiploid fraction are shown, respectively.

motes degradation of p53 (30). p16^{INK4a} is a member of the INK4 family of CDK inhibitors, which causes cell cycle arrest at G1 phase by inhibiting CDK4/6 activities (30). Meanwhile, p21$^{CIP1/WAF1}$ is a member of the Cip/Kip family of CDK inhibitors and also induces G1 arrest by inhibiting CDK2 activities. In this report, we next examined their roles in N-RasE12-induced suppression of erythropoiesis.

At first, we examined the effects of N-RasE12 on the expression of p16^{INK4a}, p19^{ARF}, and p21$^{CIP1/WAF1}$ by semiquantitative/real-time RT-PCR analyses or immunofluorescence. As shown in Fig. 5*A* and *B*, the expression of p16^{INK4a} and p19^{ARF} was induced in N-RasE12-transduced LSK cells both in mRNA and protein levels. Also, the expression of p21$^{CIP1/WAF1}$ was increased by nearly 2-fold in N-RasE12-transduced LSK cells compared with mock-transduced LSK cells (Fig. 5*C*), suggesting that the up-regulated p16^{INK4a}, p19^{ARF}, and/or p21$^{CIP1/WAF1}$ might be involved in N-RasE12-induced suppression of erythropoiesis.

To further analyze the roles of these molecules, we next introduced N-RasE12 into LSK cells isolated from p16^{INK4a}/p19^{ARF} double knock-out (KO) mice, cocultured them with MS-5, and examined the development of erythroid cells by flow cytometry. As shown in Fig. 6*A*, the frequency of CD45^{low}TER-119^{+} erythroid cells was a little lower in N-RasE12-transduced double KO cells than in N-RasE12-transduced WT cells (WT 1.8% *versus* double KO 0.8%) (*upper panels*). In addition, although the number of these erythroid cells was slightly restored in N-RasE12-transduced double KO cells compared with N-RasE12-transduced WT cells (*lower graph*), this difference was not significant.

We also introduced N-RasE12 into LSK cells isolated from p21$^{CIP1/WAF1}$-null mice. As observed in the other experiments, N-RasE12 reduced the proportion of CD45^{low}TER-119^{+} erythroid cells both in WT and p21$^{CIP1/WAF1}$-null LSK cells (Fig. 6*B*, *upper panels*). However, p21$^{CIP1/WAF1}$ deficiency partially, but significantly, restored the proportion of this fraction from 3.0 to 5.2%. In addition, surprisingly, N-RasE12 increased the number of erythroid cells in p21$^{CIP1/WAF1}$-null LSK cells compared with mock-transduced LSK cells (Fig. 6*C*, *lower graph*), indicating that p21$^{CIP1/WAF1}$ is a major regulator of N-RasE12-induced suppression of erythropoiesis.

Because the expression of p21$^{CIP1/WAF1}$ is regulated in p53-dependent and independent manners (31–33), we finally investigated the roles of p53 in N-RasE12-induced suppression of erythropoiesis with the similar experiment. As shown in Fig. 6*C*, the proportion and number of erythroid cells in mock-transduced LSK cells were reduced by p53 deficiency. In addition, p53 deficiency did not cancel the inhibition of erythroid cell development by N-RasE12. Together, these results indicate that N-RasE12 inhibits erythropoiesis through p21$^{CIP1/WAF1}$ in a p53-independent manner.

DISCUSSION

We here found that BCR-ABL suppresses erythroid cell proliferation. This finding is largely consistent with clinical features of CML, in which anemia is commonly observed and erythroid blast crisis is a rare event. Also, we found that constitutively activated Ras, but not PI3-K or STAT5, inhibits erythropoiesis and that a farnesyltransferase inhibitor, manumycin A, restores erythroid colony formation of CML patients BM cells at relatively low concentrations. These results strongly indicate that Ras is a negative regulator of erythropoiesis downstream of BCR-ABL. So far, functions of Ras in normal erythropoiesis are controversial. It was reported that Ras signaling was essential for development of erythroid progenitors (34, 35). In contrast, H-Ras$^{-/-}$, N-Ras$^{-/-}$, and double KO (H-Ras$^{-/-}$ N-Ras$^{-/-}$) mice had no apparent hematopoietic abnormality, indicating that Ras is dispensable for normal erythropoiesis (36, 37). Regarding the roles of oncogenic Ras in erythropoiesis, it was shown that oncogenic H-Ras blocks terminal erythroid differentiation (38), and that enforced expression of an active mutant of N-Ras in primitive hematopoietic cells inhibits proliferation of erythroid cells (17, 18). Our results indicate that the excessive Ras signal would inhibit erythropoiesis, though Ras signal might be to some extent necessary for erythroid cell survival. Ras is mutated in a significant proportion of cases with acute myeloid leukemia and myelodysplastic syndromes (39), or constitutively activated by various oncogenic TKs, including FLT3-ITD (2), c-KIT D816V (40), and TEL-PDGFRB (41). So, anemia observed in these hematologic malignancies also might be, at least partly, attributed to the constitutively activated Ras signal. However, in this study, JAK2 V617F slightly enhanced erythropoiesis as observed in patients with PV, whereas its downstream pathways including Ras, PI3-K, and STAT5 are common to BCR-ABL (1, 5). As for this difference, we here found that JAK2 V617F does not activate Ras signal so strongly as BCR-ABL. Also, it was speculated that JAK2 V617F would utilize mainly STAT5 to promote erythropoiesis in PV patients. Although Ras has some isoforms, we focused on N-Ras,

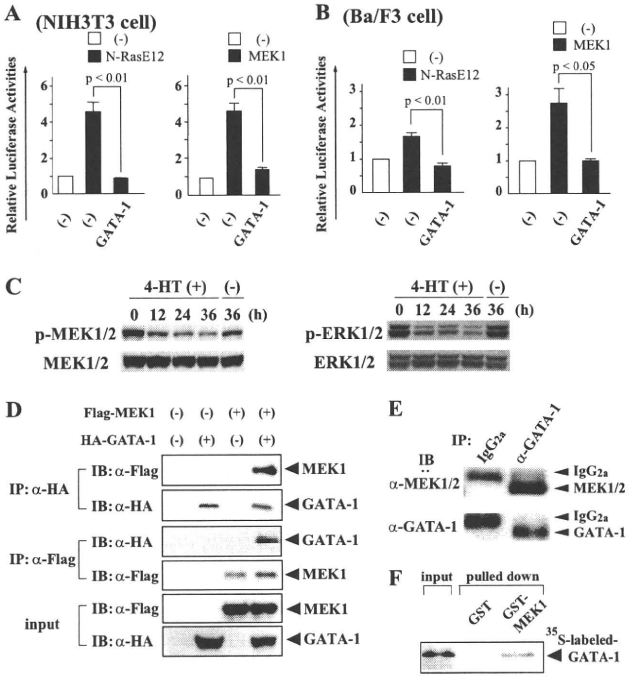

FIGURE 4. **GATA-1 blocks the Ras/Raf/MEK/ERK pathway through its direct interaction with MEK1.** *A*, NIH3T3 cells (2×10^5 cells seeded in 60-mm dish) were transfected with the indicated expression vectors and the reporter gene ($3 \times$ AP-1-Luc) together with pRL-CMV. After 12 h, the cells were serum-deprived for 24 h, then lysed, and subjected to the measurement of the firefly and *Renilla* luciferase activities. The relative firefly luciferase activities normalized by the *Renilla* luciferase activities are shown as means ± S.D. of three separate experiments. *B*, Ba/F3 cells (2×10^6 cells) were transfected with the same vectors as Fig. 4*A* using Amaxa Nucleofector technology. After 24 h of culture, the cells were lysed and subjected to the measurement of the luciferase activities. *C*, Ba/F3/N-RasE12/G1ERT cells cultured in RPMI supplemented with 1% FBS were treated with 1 μM 4-HT or vehicle. Total cellular lysates were prepared at the indicated time and subjected to immunoblotting with the indicated Abs. The filters were reprobed with corresponding Abs to confirm that the equal amounts of the proteins were loaded. *D*, coimmunoprecipitation analyses were performed using 293T cells transfected with HA-tagged GATA-1 and/or Flag-tagged MEK1 as indicated. *IP*, immunoprecipitation; *IB*, immunoblotting; α, anti. *E*, total cellular lysate was prepared from murine BM CD71$^+$ cells. Immunoprecipitation and immunoblot analyses were performed with the indicated antibodies. F. The *in vitro* binding between GATA-1 and MEK1 was examined by GST pull-down assays. ^{35}S-labeled GATA-1 was incubated with GST-MEK1 bound to glutathione-Sepharose beads, and the binding complex was separated by gel electrophoresis and subjected to autoradiography.

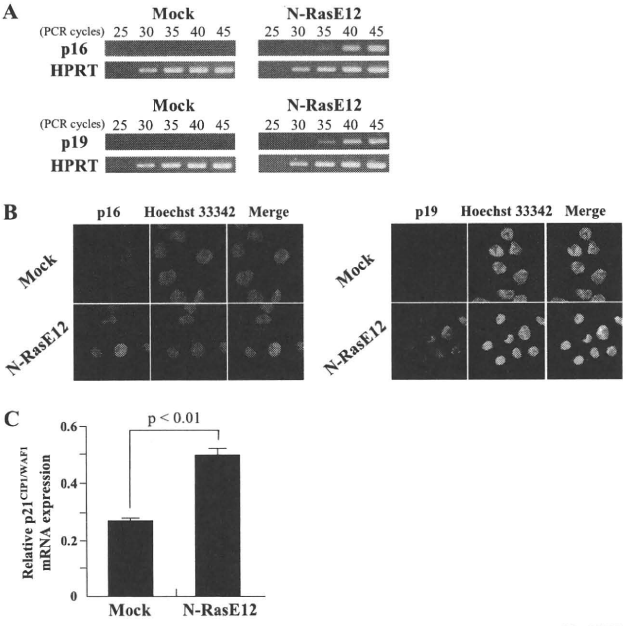

FIGURE 5. **Increase in expression levels of p16^{INK4a}, p19^{ARF}, and p21$^{CIP1/WAF1}$ by oncogenic Ras.** *A–C*, LSK cells transfected with Mock or N-RasE12 were cultured with rmSCF, rmIL-3, and rhEPO for 2 days. Total RNA was isolated from GFP$^+$ cells, and the expression levels of p16^{INK4a} and p19^{ARF} were analyzed by semiquantitative RT-PCR (*A*). Immunofluorescence staining of p16^{INK4a} and p19^{ARF} localizations (*red*) in Hoechst 33342-stained nuclei of GFP$^+$ cells are shown (magnification, 630×) (*B*). The expression levels of p21$^{CIP1/WAF1}$ were analyzed by real-time RT-PCR. The results are normalized to the levels of HPRT gene and shown as means ± S.D. ($n = 3$) (*C*).

because, in myeloid malignancies, N-Ras mutations are more frequent than K-Ras, whereas H-Ras mutations are rare (39, 42–44). It is predictable that activated N-Ras has stronger leukemogenic potential than activated H-Ras or K-Ras.

In contrast to the negative role of oncogenic Ras in erythropoiesis, Ras activation prominently enhanced the development of myeloid cells from LSK cells as observed in CML patients. To clarify the mechanism through which the active form of Ras plays different roles in the growth of hematopoietic cells according to the cell lineages (*i.e.* inhibition of erythropoiesis but promotion of myelopoiesis), we examined the role of GATA-1, which is a transcription factor mainly expressed in erythroid and megakaryocytic cells but not in myeloid cells. Ras-induced suppression of erythropoiesis can be considered to result from inhibition of proliferation of already committed erythroid progenitors, and blockage of commitment into erythroid lineage from HSCs. In this study, we found that GATA-1 inhibits MEK activity and suppresses the Ras-dependent proliferation of GATA-1-posistive cells. GATA-1 is necessary in the post-commitment stages of erythroid and megakaryocytic development, and is highly expressed after the commitment into megakaryocyte-erythrocyte progenitors (MEPs), but is scarcely expressed in HSCs (45). So, it is unlike that the interaction between GATA-1 and MEK1 is associated with the lineage determination of HSCs. On the other hand, recent reports showed that suppression of erythroid cell development by H-, K-, and N-Ras occurs at later stages of differentiation (18, 38, 46). These data are consistent with our result that GATA-1 interacts with MEK1, thereby inhibiting Ras-mediated mitogenic signals.

However, this result raises a question where these molecules interact together in the cells because GATA-1 is located in the nucleus and MEK is in the cytoplasm (47). As an explanation it was previously reported that MEK contains a nuclear export signal in its N-terminal domain, indicating that MEK is translocated to the nucleus upon mitogenic stimulation and then goes back to the cytoplasm after transduction of its signal (48). So, GATA-1 is supposed to interact with MEK1 in the nucleus, thereby inhibiting its activity. This hypothesis that GATA-1 would inhibit MEK activities is also contradictory to the fact that platelet counts are often elevated in CML patients, because MEK has been shown to be important for the maturation (polyploidization) of megakaryocytes, in which GATA-1 is highly expressed as well as in erythroid cells. Regarding this issue, Jacquel *et al.* reported that PMA-induced megakaryocytic maturation is only partly dependent on the MEK/ERK pathway and suggested the involvement of other pathways such